

Contract No:

This document was prepared in conjunction with work accomplished under Contract No. DE-AC09-08SR22470 with the U.S. Department of Energy (DOE) Office of Environmental Management (EM).

Disclaimer:

This work was prepared under an agreement with and funded by the U.S. Government. Neither the U. S. Government or its employees, nor any of its contractors, subcontractors or their employees, makes any express or implied:

- 1) warranty or assumes any legal liability for the accuracy, completeness, or for the use or results of such use of any information, product, or process disclosed; or
- 2) representation that such use or results of such use would not infringe privately owned rights; or
- 3) endorsement or recommendation of any specifically identified commercial product, process, or service.

Any views and opinions of authors expressed in this work do not necessarily state or reflect those of the United States Government, or its contractors, or subcontractors.



Stabilization of Spherical Rescorcinol Resin in Grout- Maintenance of the Hanford Integrated Disposal Performance Assessment FY 2018

Ralph L. Nichols

Kenneth L. Dixon

Daniel I. Kaplan

August 2018

SRNL-STI-2018-00342, Revision 0



DISCLAIMER

This work was prepared under an agreement with and funded by the U.S. Government. Neither the U.S. Government or its employees, nor any of its contractors, subcontractors or their employees, makes any express or implied:

1. warranty or assumes any legal liability for the accuracy, completeness, or for the use or results of such use of any information, product, or process disclosed; or
2. representation that such use or results of such use would not infringe privately owned rights; or
3. endorsement or recommendation of any specifically identified commercial product, process, or service.

Any views and opinions of authors expressed in this work do not necessarily state or reflect those of the United States Government, or its contractors, or subcontractors.

Printed in the United States of America

**Prepared for
U.S. Department of Energy**

Keywords:

Ion Exchange Resin

Grout

Performance Assessment

Hydraulic Conductivity

Water Retention

Partition Coefficient

Retention: *Permanent*

Stabilization of Spherical Rescorcinol Resin in Grout- Maintenance of the Hanford Integrated Disposal Performance Assessment FY 2018

Ralph L. Nichols
Kenneth L. Dixon
Daniel I Kaplan

August 2018

Prepared for the U.S. Department of Energy under
contract number DE-AC09-08SR22470.

REVIEWS AND APPROVALS

AUTHORS:

Ralph L. Nichols, Geosciences	Date
-------------------------------	------

Kenneth L. Dixon, Geosciences	Date
-------------------------------	------

Daniel I Kaplan, Environmental Sciences & Biotechnology	Date
---	------

TECHNICAL REVIEW:

Gregory P. Flach, Environmental Restoration Technology Section	Date
--	------

Christine. A. Langton, Waste Form Processing Technologies	Date
---	------

APPROVAL:

Nancy V. Halverson, Manager, Geosciences Geosciences	Date
---	------

John J. Mayer II, Manager, Environmental Sciences & Biotechnology Date	
---	--

E. E. Brown, WRPS CTO	Date
-----------------------	------

PREFACE OR ACKNOWLEDGEMENTS

The authors would like to acknowledge the contributions of the laboratory staff that provided essential support for this effort (Katie Hill, Vickie Williams, and Courtney Burckhalter), Ken Gibbs, Michael Summer, and Ross Smith for the support with visual examination of the samples, and James Dyer for internal reviews and technical checking of the data and calculations.

The testing and analysis of heat hydration by Devon McClane is greatly appreciated by the authors.

The authors also appreciate the support and feedback from WRPS CTO (Elvie Brown, Matt Landon and Dave Swanberg) and the IDF PA team from WRPS (Pat Lee) and Intera (Bob Andrews and team). These contributions helped to focus the efforts on areas expected to provide the most benefit for the IDF Performance Assessment efforts.

EXECUTIVE SUMMARY

Washington River Protection Solutions (WRPS) commissioned the Savannah River National Laboratory (SRNL) (Brown, 2016) to develop and implement a testing program to support the findings presented in the SSW data package for the Integrated Disposal Facility Performance Assessment (IDF PA) (Flach et al., 2016a). The specific objectives of the work in this report are to;

- measure fresh and cured properties of a grouted waste form consisting of cementitious material and spherical resorcinol formaldehyde cation exchange resin
- measure the partition coefficient of technetium and iodine in grout matrices

This report presents results from the work on this project completed by SRNL in FY17.

Operation of the low activity waste vitrification facility (LAW) part of the Waste Treatment and Immobilization Plant (WTP) at Hanford will generate several solid secondary waste (SSW) streams including used process equipment, contaminated tools and instruments, decontamination wastes, high-efficiency particulate air filters (HEPA), carbon absorption beds, silver mordenite iodine sorbent beds, and spent ion exchange resins (IXr), all of which are to be disposed of in the Integrated Disposal Facility (IDF). The baseline treatment method in the IDF Performance Assessment (PA) for SSW is solidification/stabilization using cementitious material. The Hanford Mix 5 has been identified as the baseline grout for encapsulation of debris SSW (HEPA filters) and solidification/stabilization of non-debris SSW (carbon absorption beds, silver mordenite iodine sorbent beds, and spent ion exchange resins). Hanford Mix 5 is a blend of ASTM (C150-18) Type I-II cement (OPC), Class F fly ash (FA), water, BASF Pozzolith 80 and BASF Master Fiber M100 (fiber) that is currently used for disposal of debris in carbon steel containers (B25) in Hanford's 200 West Area Low Level Waste Burial Ground trenches.

This report documents the results of studies performed by the SRNL to evaluate (1) the stabilization of spherical resorcinol formaldehyde (sRF) resin, a cation exchange resin in grout consisting of OPC, FA, and blast furnace slag (BFS) and (2) retention of ^{99}Tc and iodine in grout. Three different mixes of cementitious material (CM) were tested including the Hanford Grout Mix 5. The CM mixes tested contained 75:25:0 (Hanford Grout Mix 5), 45:10:45 and 20:5:75 wt% of FA:OP:BFS and H_2O :CM 0.29, 0.45, and 0.45 respectively. H_2O :CM was adjusted as necessary meet fresh property guidelines. Only Hanford Grout Mix 5 used admix and fiber. Neither of the mixes containing BFS had admixes or fiber. Batches of each grout mix were prepared containing 10% and 30% volume fraction drained sRF resin. Selected fresh (flow, bleed, set time, and heat of hydration) and cured (hydraulic conductivity, water retention characteristics, compressive strength, dry bulk density, and porosity) properties were tested on waste forms from each of the formulations. Guideline for flow, bleed, and compressive strength were established for this study. The resulting waste forms met guidelines selected for fresh (flow and bleed) and cured properties (compressive strength). Additionally, hydraulic properties were similar to those recommended in the Solid Secondary Waste Data Package Supporting Hanford Integrated Disposal Facility Performance Assessment by Flach et al. (2016b).

Preliminary results from baseline scenarios of the IDF PA indicate that ^{99}Tc and ^{129}I may be the risk drivers. Adsorption and desorption tests were conducted to determine site specific ^{99}Tc and ^{129}I partition coefficient (K_d) values for these constituents of potential concern (COPC). The ^{99}Tc K_d determined in the study for two mixes (w and w/o BFS) are higher than those recommended by Flach et al. (2016a) for the IDF PA. Partition coefficients for ^{129}I are similar to those recommended by Flach et al. (2016a) for the IDF PA. IO_3^- and organic-I had higher K_{ds} than I for the same grout.

TABLE OF CONTENTS

LIST OF TABLES	ix
LIST OF FIGURES	x
1.0 Introduction	1
2.0 Background	1
2.1 Conceptual Model for Waste Form Process	3
3.0 Experimental Procedure	4
3.1 Grout Stabilized sRF Resin	4
3.1.1 Fresh Properties	7
3.1.1.1 Free Liquids/Standing Water	7
3.1.1.2 Grout Flowability	8
3.1.1.3 Heat of Hydration	8
3.1.1.4 Set Time	9
3.1.2 Cured Properties	9
3.1.2.1 Saturated Hydraulic Conductivity	9
3.1.2.2 Density and Porosity	10
3.1.2.3 Water Retention	10
3.1.2.4 Compressive Strength	12
3.1.2.5 Dimensional Stability	12
3.2 Radionuclide Retention in Grout	13
3.2.1 ⁹⁹ Tc Partitioning Coefficients	14
3.2.2 Iodine Partition Coefficient	14
3.2.2.1 Iodine Desorption	15
3.2.2.2 Iodine Adsorption	15
3.2.2.3 Iodine Speciation	15
4.0 Results	16
4.1 Grout Stabilized sRF Resin	16
4.1.1 Incorporation of sRF Resin into Grout	16
4.1.2 Formulation Refinement	19
4.1.3 Drained sRF Resin Water Content	20
4.1.4 Fresh Properties	21
4.1.4.1 Grout Flow	21
4.1.4.2 Set	21
4.1.4.3 Bleed	22

4.1.4.4 Heat of Hydration.....	22
4.1.5 Cured Properties.	23
4.1.5.1 Hydraulic Conductivity.....	23
4.1.5.2 Density and Porosity	23
4.1.5.3 Moisture Retention.....	24
4.1.6 Compressive Strength.....	28
4.1.7 Dimensional Stability	29
4.2 Radionuclide Retention in Grout.....	29
4.2.1 ⁹⁹ Tc Uptake by Grout Under Partially Reducing Conditions.....	30
4.2.2 Iodine Partition Coefficient	32
4.2.2.1 Iodine Adsorption	32
4.2.2.2 Iodine Desorption.....	33
5.0 Conclusions.....	36
6.0 References.....	39

LIST OF TABLES

Table 1 Mixes and sRF Resin loading studied in Phase 2.	4
Table 2 Composition of cementitious materials used in this study.....	6
Table 3 Fresh and cured properties measured in this study.	7
Table 4 Salts used in constant vapor pressure method for moisture retention characteristics.	12
Table 5 Formulation of mixes used to study radionuclide retention in grout.	13
Table 6 Mixes used in simulated waste forms.	19
Table 7 Results from x-ray fluorescence analysis of Mix 1, Mix 5, and Mix 13.....	20
Table 8 Water content of resin used in final batches.	21
Table 9 Water content of resin received from AVANTech.	21
Table 10 Flow properties of grouted sRF resin waste forms.	22
Table 11 Heat of Hydration results for mixes prepared.	23
Table 12 Cured properties for simulated waste forms.	24
Table 13 Van Genuchten curve fitting parameters for simulated waste forms in this study.	25
Table 14 Aqueous chemistry of leaching solution and leachate.	30
Table 15 Reduction potential of raw solid materials used to make Cast Stone using the of ingredients used in wasteforms at SRS and Hanford.....	31
Table 16 Iodine sorption experiments by grout with and without slag in formulation: iodine aqueous speciation and K_d values after 7-day equilibration period.	33
Table 17 Total iodine, organic and inorganic carbon content of grout from Mix 1.0 and Mix 13.0 after 28 day cure.....	33
Table 18 Desorption K_d values (mL/g) as a function of grout formulation and iodine species added to mix prior to curing.	35
Table 19 Comparison of K_d values measured in this report vs. those recommended in the SSW IDF data package (Flach et al. 2016).	38

LIST OF FIGURES

Figure 1 Cation exchange resin stabilized in grout.	1
Figure 2 Ternary diagram showing cementitious material blends used in this study.	2
Figure 3 Conceptual model for solidifying drained sRF resin.	3
Figure 4 Overhead mixer blending sRF resin with cementitious material and water.	5
Figure 5 Measurement of flow to determine flowability	8
Figure 6 Grouted sRF resin waste form loaded in flexible wall permeameter.	9
Figure 7 Grout wafers used in the CVP method equilibrating in a sealed desiccator containing a saturated salt solution.	11
Figure 8 Grout prisms for dimensional stability testing (a) prism in curing mold, (b) comparator for measuring prism length.	13
Figure 9 Simulated waste form with 0.2 v/v sRF resin loading Mix 1.2 grout, (a) macroscopic photograph and (b) μ CT slice.	17
Figure 10 Scanning electron micrograph (a) and energy dispersive x-ray spectra (b) of sRF resin particle stabilized in grout where yellow is paste and red is sRF particle sRF resin stabilized in grout.	18
Figure 11 Ternary diagram showing mix designs used in this study.	20
Figure 12 Probability Density Function for materials presented in the initial data package (Flach et. al. 2016) and results for individual grout samples and simulated waste forms containing sRF resin.	24
Figure 13 Water desorption curves for simulated waste forms (a) Flach et. al. [4], (b) 1.1 and 1.3, (c) 5.1 and 5.3, (d) 13.1 and 13.3. Note: xx.y = Mix#.sRF loading.	26
Figure 14 Capillary tube model for pore network in a grouted waste form	27
Figure 15 Relative hydraulic conductivity curves for grout sRF resin (a) Flach et al. (2016a), (b) Mix 1, (c) Mix 5, and (d) Mix 13.	28
Figure 16 Compressive strength of grouted waste forms with increasing amounts of sRF resin.	29
Figure 17 T_c K_d values measured under benchtop conditions as a function of contact time of the three grout mixes.	30
Figure 18 ^{99}Tc K_d values from the equilibrium K_d Test (3 replicates, 14-day equilibrium time, 2:1 grout leachate, 1:5 grout:leachate; measured under benchtop conditions).	32
Figure 19 Desorption of iodine from crushed Mix 1.0 and Mix 13.0. Error bars were calculated from duplicate samples and include propagation of analytical error. Error bars may be hidden by symbol.	34
Figure 20 Comparison of desorption K_d for mixes amended with different forms of iodine.	35

LIST OF ABBREVIATIONS

3d-μCT	Three Dimensional Micro Computed Tomography
B25	Carbon Steel Container
BFS	Blast Furnace Slag
CM	Cementitious Material
COPC	Constituent of Potential Concern
CTO	Chief Technology Office
CVP	Controlled Vapor Pressure
DOE	Department of Energy
FA	Fly Ash
FWP	Flexible Wall Permeameter
FY	Fiscal Year
GC-MS	Gas Chromatograph – Mass Spectrometer
HEPA	High-Efficiency Particulate Air
HLW	High-Level Waste
IDF	Integrated Disposal Facility
ITZ	Interfacial Transition Zone
IXr	Ion exchange resin
Kd	Distribution coefficient
MPa	Megapascal
LAW	Low-Activity Waste
LSW	Liquid Secondary Waste
n/a	Not applicable
OPC	Ordinary Portland Cement
PA	Performance Assessment
PDF	Probability Distribution Function
SEM-EDX	Scanning Electron Microscopy – Energy Dispersive X-ray Spectrograph
sRF	Spherical Resorcinol Formaldehyde
SRNL	Savannah River National Laboratory
SSW	Solid Secondary Waste
vG	van Genuchten
v/v	Volume/volume
WRC	Water Retention Curve
WRPS	Washington River Protection Solutions
WTP	Waste Treatment and Immobilization Plant
XRF	X-ray Fluorescence

1.0 Introduction

Washington River Protection Solutions (WRPS) commissioned the Savannah River National Laboratory (SRNL) (Brown, 2016) to develop and implement a testing program to support the findings presented in the SSW data package for the Integrated Disposal Facility Performance Assessment (IDF PA) (Flach et al., 2016a). This included developing and implementing a strategy for determining properties of SSW to support maintenance of the IDF PA. The specific objectives of the work in this report are to;

- measure fresh and cured properties of a grouted waste form consisting of cementitious material and spherical resorcinol formaldehyde cation exchange resin
- measure the partition coefficient of technetium and iodine in grout matrices

This report presents results from the work on this project completed by SRNL in FY17.

2.0 Background

The Waste Treatment and Immobilization Plant (WTP) at Hanford is being constructed to treat 56 million gallons of radioactive waste currently stored in underground tanks at the Hanford site. This treatment includes vitrification of high-level waste (HLW) and low activity waste (LAW) fractions. Operation of the LAW Vitrification facility will generate several solid secondary waste (SSW) streams including used process equipment, contaminated tools and instruments, decontamination wastes, high-efficiency particulate air filters (HEPA), carbon absorption beds, silver mordenite iodine sorbent beds, and spent ion exchange resins (IXr), all of which are to be disposed of in the Integrated Disposal Facility (IDF). The IXr is expected to contain low concentrations of ^{99}Tc and ^{129}I following final elution and dewatering in preparation for disposal. The HEPA filters, carbon absorption beds, silver mordenite iodine sorbent beds, and spent IXr are expected to be stabilized using cementitious material (CM) prior to disposal (Flach et al., 2016a). Figure 1 shows an example of IXr stabilized in grout.



Figure 1 Cation exchange resin stabilized in grout.

Currently, debris disposed of in Hanford's 200 West Area Low Level Waste Burial Ground trenches is typically placed in a 4x4x6 ft carbon steel container (B25) and encapsulated with a grout commonly referred to as "Hanford Mix 5", also referred to as American Rock Products 4257020-Perma-Fix Grout 2500 PSI [0] (Tomlinson, 2016). Hanford Mix 5 contains ASTM (C150-18) Type I-II cement (OPC), Class F fly ash (FA), water, BASF Pozzolith 80 and BASF Master Fiber M100 (fiber). Pozzolith is included in concrete mixes to reduce the amount of water needed in mixing and retard setting time. MasterFiber M100 is used to reduce shrinkage cracking.

The grout is mixed at a batch plant and transported via concrete truck (transit mixer) to the Perma-Fix facility where it is poured into a B25 box containing debris. The grout cures in the B25 box uncovered for ~ 72 hours prior to being covered and transported to the Hanford 200 West Area Low Level Waste Burial Ground for disposal. If bleed water is noticed at the end of the 72-hour holding period, diatomaceous earth is added to the surface of the grout to sorb the free liquid prior to being covered. Ventilation is the only environmental control for the process and the storage room where the 72-hour curing occurs. No fresh properties are measured during batching or placement of the grout and there are no technical requirements for the fresh or cured grout used to solidify debris for disposal in the Hanford 200 West Area Low Level Waste Burial Ground trenches.

The Hanford Mix 5 has been identified as the baseline grout for encapsulation of debris SSW (HEPA filters) and solidification/stabilization of non-debris SSW (carbon absorption beds, silver mordenite iodine sorbent beds, and spent ion exchange resins). Flach et al. (2016a) compiled the results of testing 98 samples from 13 different CM mixes to determine physical properties related to moisture flow and solute transport such as hydraulic conductivity, moisture retention, and diffusion coefficients. Figure 2 is a ternary diagram showing the various ratios of CM in the mixes analyzed in Flach et al. (2016a).

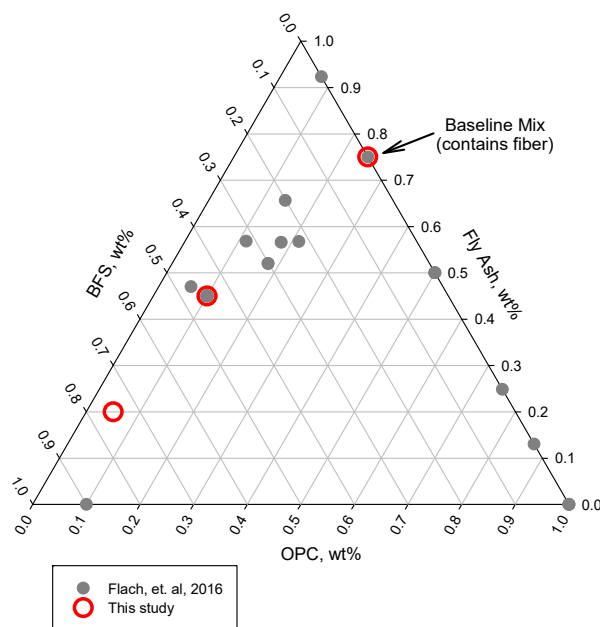


Figure 2 Ternary diagram showing cementitious material blends used in this study.

SRNL conducted testing of 13 different grout mixes including Hanford grout Mix 5 to obtain data for use in identifying candidate mixes of CM for further testing in use to stabilize SSW. The results from these tests are reported in Nichols et al. (2017). Three mixes were selected from those tested in Nichols et al. (2017) for further testing in the solidification of spherical resorcinol formaldehyde (sRF), a cation IXr

proposed for the removal of $^{137}\text{Cs}^+$ from liquid radioactive wastes processed at the WTP. Spent sRF resin is expected to contain low concentrations of ^{99}Tc and ^{99}I following final elution and dewatering in preparation for disposal. The base mix used in the Hanford Low Level Burial Ground and 2 additional CM mixes containing blast furnace slag (BFS) were selected for testing. Mixes that contain BFS produce reducing grouts which improves the retention of ^{99}Tc . Figure 2 compares the CM blends selected for this study with those identified in Flach et al. (2016a).

Discussions were held with WRPS Chief Technology Office (CTO) staff to address the form of the sRF resin that would require stabilization. The expectation is that the sRF resin will be in a H^+ form, but not the original bead diameter ($\sim 360\text{ }\mu\text{m}$). After multiple elution cycles, the resins are expected to be slightly larger ($\sim 385\text{ }\mu\text{m}$). Initial testing was conducted starting with the eluted H^+ form. Lafond et al. (2015) has shown that the IXrs exhibit a transient swelling of small magnitude due to the decrease in the osmotic pressure of the external solution. In order to consider the most straightforward operational approach, no pretreatment of SRF resin was incorporated for the testing.

2.1 Conceptual Model for Waste Form Process

The process for blending non-debris material into the grout from the WTP has not been developed. A conceptual model, Figure 3, for this process was developed from conversations with WRPS, American Rock Products Richland Plant and the Perma-Fix Office in Richland.

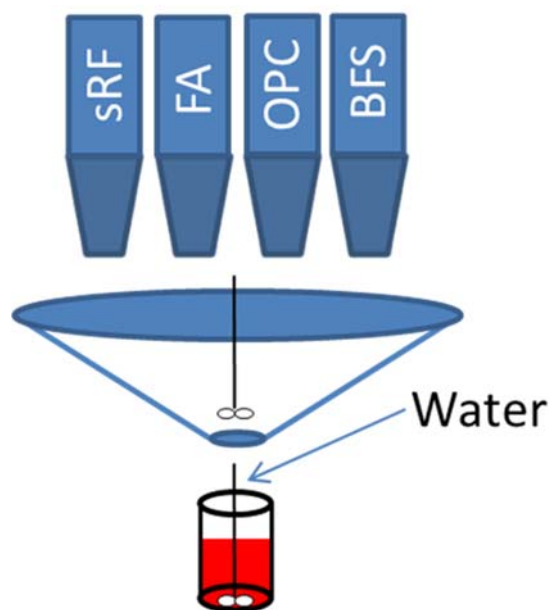


Figure 3 Conceptual model for solidifying drained sRF resin.

The following conceptual flow sheet for the blending process was developed based on these conversations:

1. Drain eluted/rinsed ion exchange resin and store in High Integrity Container (IC) prior to solidification
2. Add appropriate amount of water to drum
3. Add ion exchange resin and mix with water
4. Add cementitious material to drum and mix moving beater up and down as necessary
5. Add admixtures to drum and mix moving beater up and down as necessary
6. Stage drum uncovered in process area for 72 hours
7. After 72 hours, add diatomaceous earth to surface of grout if bleed water is present, cover drum and place drum in storage area awaiting transport to IDF

Preliminary results from baseline scenarios of the IDF PA indicate that ^{99}Tc and ^{129}I may be the risk drivers. Adsorption and desorption tests were conducted to determine site specific partition coefficients (K_d) values for these constituents of potential concern (COPC). This report contains results from FY 2017 testing of simulated waste forms prepared from drained sRF resin and CM and K_{ds} for ^{99}Tc and ^{129}I in grout.

3.0 Experimental Procedure

3.1 Grout Stabilized sRF Resin

Grout stabilized sRF resin waste forms were prepared using drained sRF resin from previous mechanical property tests (WRPS, 2016), cementitious material (CM), water and admixes. Three different grouts and two different sRF loadings were selected for testing, Table 1. Figure 2 compares the CM used in this study with those used in the IDF PA data package prepared by Flach et al. (2016a). Cementitious materials used to prepare the simulated waste forms consisted of type-I/II Portland cement (OPC; Ash Grove Cement West Inc., Durkee, OR), Class-F fly ash (FA: LaFarge North America Inc., Pasco, WA), Grade-120 blast furnace slag (BFS; LaFarge North America Inc., Pasco, WA), admix BASF Pozzolith 80 and BASF Master Fiber M100 from samples provided by American Rock Products, Lafarge Northwest, and BASF. The elemental composition of the cementitious materials used in this study was determined using x-ray fluorescence; XRF results are presented in Table 2. Samples for XRF are dried at 105°C and then heated to 1000°C to determine loss on ignition (LoI). Following LoI determination the remaining material is prepared using lithium tetraphenylborate prior to XRF. Results are normalized to 100% including LoI. XRF is calibrated using matrix match standards.

In Table 1 Mix 1.# is the baseline mix in the IDF PA. Mix 5.# has the highest BFS content and preliminary data from Phase 1 (Nichols et al., 2017) indicate it has low hydraulic conductivity when compared to other mixes with 0.75 w/w content BFS. Mix 13.# was selected to include a grout with mid-range BFS content (0.45 w/w) in the CM and has well established properties. Mix 13 has been tested extensively with alkaline salt solutions simulating LAW as well as Hanford liquid secondary waste (LSW).

Table 1 Mixes and sRF Resin loading studied in Phase 2.

Mix	H2O:CM (w/w)	FA/OPC/BFS (w/w)	sRF Resin Loading (v/v)
1.0	0.29	75/25/0	0.0
1.1	0.29	75/25/0	0.1
1.2	0.29	75/25/0	0.2
1.3	0.29	75/25/0	0.3
5.0	0.45	20/5/75	0.0
5.1	0.45	20/5/75	0.1
5.3	0.45	20/5/75	0.3
13.0	0.45	45/10/45	0.0
13.1	0.45	45/10/45	0.1
13.3	0.45	45/10/45	0.3

Note: Mix 1.0 is baseline Hanford Grout Mix 5, $v/v = v_{\text{sRF}}/v_{\text{total}}$

Mix 1 also includes $5.8\text{e-}04 \text{ g/g}_{\text{grout}}$ admix BASF Pozzolith 80 and $1.25\text{e-}02 \text{ g/g}_{\text{grout}}$ BASF Master Fiber M100. Mix 5 and Mix 13 do contain either admix BASF Pozzolith 80 and BASF Master Fiber M100

Waste forms were prepared by mixing drained sRF resin with a predetermined amount of water based on $\text{H}_2\text{O:CM}$ for the specific mix in a beaker using an overhead mixer. Once the drained sRF resin and water were blended and mixed for two minutes the CM was added to the beaker containing water and drained sRF resin as it was being stirred by an overhead mixer, Figure 4. Mixer speed was adjusted to maintain a vortex in the grout as CM was added. Once all the CM was included, the admix and fiber (Mix 1.0, 1.1, and 1.3 only) were added. Fiber was shredded by hand using tweezers to break up the fiber into smaller assemblages prior to adding to the grout to simulate the effect of gravel in fiber in typical concrete mixes. After all ingredients were in the grout, the grout was stirred until an overall mixing period of 15 minutes had been completed while ensuring there was a vortex at all times. This mixing method was developed to mimic an in-container solidification process illustrated in Figure 3 that may be used to solidify sRF resin and is similar to a mixing procedure developed by SRNL to standardize sample preparation for grout testing studies. Occasionally the mixer was stopped to “burp” the grout to remove air pockets that affect mixing. Once the mixing was completed the grout was immediately decanted for fresh property testing and into molds for curing.



Figure 4 Overhead mixer blending sRF resin with cementitious material and water.

AVANTech, Inc., located in Columbia, SC, conducted full scale performance testing of sRF resin including the dewatering technology proposed for the system (WRPS, 2016). Spent material from the full-scale sRF resin testing was collected for use in this study and stored in pH adjusted water in its H^+ form so it would closely resemble spent sRF resin that is expected to be disposed of as SSW in the IDF. The dewatering technology was not tested until performance tests were complete and therefore dewatered sRF resin was not available for inclusion in sRF waste forms prepared for this study. AVANTech, Inc. provided samples of drained sRF resin, that had been previously used in full scale testing to determine Cs^+ removal, for determination of gravimetric water content using the same method employed for this study.

Table 2 Composition of cementitious materials used in this study.

	Cement	Flyash	Blast Furnace Slag
CaO, wt%	63.9	13.1	41.1
SiO ₂ , wt%	20.1	48.5	32.4
Al ₂ O ₃ , wt%	4.9	17.9	14.6
Fe ₂ O ₃ , wt%	3.3	6.5	0.8
SO ₃ , wt%	3.1	0.6	2.5
MgO, wt%	0.9	5.4	5.3
K ₂ O, wt%	0.3	1.7	0.3
TiO ₂ , wt%	0.3	1.1	0.6
Na ₂ O, wt%	0.3	3.7	0.2
SrO, wt%	0.1	0.3	0.1
P ₂ O ₅ , wt%	0.1	0.3	0.0
Mn ₂ O ₃ , wt%	0.0	0.1	0.2
LoI, wt%	2.7	0.8	1.9

Note: LoI = Material lost on ignition at 1000°C.

The spent sRF resin used in simulated waste forms was drained prior to mixing using a disposable filter unit that had a 500 mL upper chamber and 0.45µm nylon filter. A predetermined bulk volume of sRF resin was decanted into the upper filter chamber and allowed to gravity drain for 3-4 hours. Following drainage, a small sample of drained sRF resin was removed for drying in an oven at 105°C to determine gravimetric water content and the remainder was used to prepare the simulated waste form. Samples were periodically removed from the oven and weighed until two consecutive weights were within $\pm 0.5\%$. The actual volume of resin used in the simulated waste forms was calculated using the gravimetric water content of the sRF resin and the sRF dry particle density.

A trial waste form (Mix 1.2, Table 1) was prepared prior to the waste forms used for testing to assess the method for preparing the waste forms and incorporation of sRF resin in the cured waste form. An sRF resin loading of 0.2 v/v was used with Mix 1 to prepare the simulated waste form and evaluate how well the sRF resin would stay mixed in the grout while it cured. The trial waste form was prepared prior to preparing waste forms with 0.1 and 0.3 v/v sRF resin.

Fresh and cured physical and hydraulic properties, Table 3, of waste forms containing 0.1 and 0.3 v/v sRF resin were evaluated to compare with the 2016 data package and support decisions to down-select from the range of mix options in this study.

Table 3 Fresh and cured properties measured in this study.

Property	Comments
Fresh Properties	
Grout Flow	Property related to workability i.e. and how well a grout would flow around objects when used for encapsulation, self-leveling.
Heat of Hydration	Gauge the onset and extent of hydration reactions and maintain temperature limits as the waste form cures.
Set Time	Used to assess when a concrete has hardened sufficiently and is no longer deformable.
Free Liquids	Also referred to as bleed, is an indication of potential settlement of heavier cementitious material resulting in free liquids on the surface and the time to incorporate the free liquid.
Cured Properties	
Density	Input for transport calculations in Performance Assessment.
Porosity	Input for transport calculations in Performance Assessment.
Compressive Strength	Used to ensure waste form will survive forces from transportation and disposal and provide stability to disposal system.
Saturated Hydraulic Conductivity	Input for flow calculations in Performance Assessment.
Moisture Retention	Input for flow calculations in Performance Assessment.

3.1.1 Fresh Properties

3.1.1.1 Free Liquids/Standing Water

Standing liquid of freshly prepared grout was determined by measuring the residual liquid remaining after 72 hours using a modified version of ASTM (C 232-04) described in J.H. Westsik et al. (2013). Fresh grout is placed in a sample container and weighed. Samples were then stored in a zip top bag with a moist towel to maintain a humid environment and mitigate any potential losses from evaporation. Free water was decanted into a container after 72 hours and weighed. The volume of the residual liquid was calculated from the measured mass of the liquid recovered from the sample (J.H. Westsik et al., 2013). The density of the liquid was assumed to be the same as the water to prepare the mix. The standing liquid calculation is reported as the volume of fluid collected over the volume of hardened grout calculated from the mass of the sample. Standing liquid present in the sample is a preliminary indication that settling may have occurred. This may be an indication of preferential settling (segregation). Residual liquid may also be reabsorbed with time.

3.1.1.2 Grout Flowability

The flow test provides information regarding workability and was the first fresh property measured. The results were used to determine if the batch was suitable for continued testing. Flow was determined by placing a stainless-steel cylinder (4.3cm inside diameter x 7.7cm long) open on both ends on a stainless-steel plate and filling it completely full with grout immediately after mixing. Once the cylinder was full it was quickly lifted straight up to release the grout onto the stainless-steel plate forming a “pancake” as shown in Figure 5. The diameter of the pancake was then measured using a caliper. Grout with a flow ≥ 120 mm was considered workable for this study. A flow of ≥ 120 mm was selected based on measurements of the grout batches prepared using the baseline cementitious material mix, which is known to be acceptable for current applications at Hanford. This method is modified from ASTM (D 6103 – 04) by using a smaller cylinder based on previous experience with grouts (Cozzi et al., 2013)



Figure 5 Measurement of flow to determine flowability

3.1.1.3 Heat of Hydration

The isothermal heat of hydration for the sRF resin waste forms was measured in accordance with (ASTM, C 1679-09) Standard Method for Measuring Hydration Kinetics of Hydraulic Cementitious Mixtures Using Isothermal Calorimetry (ASTM, C 1679-09). This measurement is used to compare the hydration kinetics of sRF resin waste forms made from different CM blends and different sRF resin loading. The composition of the cementitious materials as well as the composition and amount of additives can affect the magnitude and timing of hydration heat development. In large pours, the energy (heat) produced can alter the mineralogy and microstructure developed in the waste form and influence cured properties.

An eight-channel isothermal calorimeter (TAM Air, TA Instruments, Newcastle, DE) was used to collect the heat generation rate and total energy of each of the mixes. Each channel consists of a twin configuration with one side for the sample and the other side for the reference material. The reference channel was balanced with 20 g of quartz sand to approximate the heat capacity of the mixes. The isothermal calorimeter was maintained at 25°C for the entirety of the testing. A sample of the fresh mix was immediately transferred to the calorimeter following preparation and the test initiated. The total energy produced, normalized per gram of dry blend material was determined for the first 72 hours of curing. The maximum generation rate (heat flow) and the elapsed time to attain this rate were also determined. Dry blend components (OPC/BFS/FA) each participate in the hydration reaction to different extents.

3.1.1.4 Set Time

Set time of freshly prepared grout was measured using ASTM (C 191-13). For this testing, the final set described in the ASTM procedure was modified to allow for up to 2 mm of penetration. The modification from the ASTM method is derived from the utilization of the data. The ASTM method is often used to determine when a pour can be walked on by the average worker. For waste form testing, the 2 mm set is an indication that sufficient structure was developed such that a waste container could be moved without disturbing the contents and was selected for consistency with (J.H. Westsik et al., 2013) where it was used to determine set time for waste forms made by immobilization of Hanford LAW using CM. The time unit for measurement is in hours, or fractions thereof. The Vicat penetration, mm, reported is after 72 hours unless otherwise noted. Seventy two hours was selected based on the conceptual model for solidification of sRF resin and the process used for solidification of debris in the Hanford 200 West Area Low Level Waste Burial Ground. Set time corresponds to the development of structure from hydration and may be used as a process control point for the transport of waste packages.

3.1.2 Cured Properties

3.1.2.1 Saturated Hydraulic Conductivity

Saturated hydraulic conductivity was measured after a minimum 28 days curing time. Samples were maintained in a sealed bag containing a moist towelette during the curing period. Simulated waste forms were removed from molds and stored in water under a vacuum prior to testing. A flexible wall permeameter (FWP) was used to measure saturated hydraulic conductivity (K_{sat}) of unmolded samples 5 cm in diameter and 10 cm long using ASTM (D 5084-10). Cut, unmolded samples were put in a container of water and placed in a vacuum chamber for ≥ 7 days. Vacuum saturated samples were loaded in the FWP and then equilibrated under a confining pressure of 5.5 bar and pore pressure of 4.8 bar. After equilibration, a pressure gradient of 0.34 bar was applied to measure hydraulic conductivity. Figure 6 shows a grouted sRF resin waste form loaded into a test cell. A latex membrane separates the sample from surrounding water used to apply a confining pressure. Upper and lower platens are used to secure the membrane to the sample and to supply fluid to the top and bottom of the sample for testing. Flow through the sample resulting from the pressure difference across the sample is measured using burettes. The pressure gradient, measured flowrate and sample dimensions are then used to calculate K_{sat} .



Figure 6 Grouted sRF resin waste form loaded in flexible wall permeameter.

3.1.2.2 Density and Porosity

Dry bulk density, ρ_b , and porosity n , were determined on cylindrical samples that had been previously vacuum saturated and tested in a flexible wall permeameter. Saturated samples were measured (diameter and length) and weighed following removal from the FWP and then placed in a 105°C oven to dry. Samples were periodically (~daily) removed from the oven and weighed until two consecutive weights were within $\pm 0.5\%$. Dry bulk density and porosity were determined using measured dimensions and weights (wt. of saturated and dry cylinder). Porosity is determined by dividing the volume of water removed from a saturated sample during drying by the total volume of the cylinder and ρ_b is determined by dividing the final dry weight of the sample by the total volume of the cylinder.

3.1.2.3 Water Retention

The water retention characteristics of grouts similar to those proposed for the disposal of SSW in the IDF are commonly represented by water retention curves (WRC) based on a closed form equation published by van Genuchten (1980) equation 1.

$$S_e(h) = \left[\frac{1}{1 + (\alpha h)^n} \right]^m \quad (1)$$

S_e	effective saturation, $\text{cm}^3 \text{H}_2\text{O} / \text{cm}^3 \text{void}$
h	pressure head, $\text{cm H}_2\text{O}$
α	inverse of the air-entry pressure, $\text{cm H}_2\text{O}^{-1}$
n	measure of the pore-size distribution, dimensionless
m	$1 - 1/n$ (Mualem, 1976)

A controlled vapor pressure (CVP) method was used to create the various levels of negative pressure head ($-h$), referred to hereafter as, suction, necessary to determine the desorption water retention curves for grout waste forms. Wafers, 1.25 cm thick, were cut from 5 cm diameter monoliths using a wet band saw and vacuum saturated prior to moisture retention testing. Vacuum saturated wafers were placed above a saturated salt solution inside a sealed container as shown in Figure 7. The saturated salt solution produces a constant relative humidity (RH) in the headspace of the sealed container.

At equilibrium the suction in the wafers can be calculated from the equilibrium RH using the Kelvin equation (2) (Nimmo and Winfield, 2002) and (Baroghel-Bouny et al., 1999). Each initially saturated wafer drains by evaporation until the suction in the sample is at equilibrium with the vapor pressure in the headspace of the container. At equilibrium, the material is assumed to attain the same total potential as the vapor in the headspace of the container (Nimmo and Winfield, 2002). This CVP method produces experimental data that can be used for determining the parameters for a desorption van Genuchten (vG) curve, equation 1. Table 4 contains the data for the salts used in this study.

$$h = -\frac{\rho_l RT}{M_v} \ln(H) \quad (2)$$

where:

h	suction (capillary pressure), Pa
ρ_l	density of water, kg/m ³
R	ideal gas constant, J/mol/°K
T	absolute temperature, °K
M_v	molar mass of water, kg/mol
H	relative humidity, unitless



Figure 7 Grout wafers used in the CVP method equilibrating in a sealed desiccator containing a saturated salt solution.

Each wafer was weighed prior to placing it in the sealed container with the salt solution. Periodically, the samples were removed and weighed to determine whether equilibrium had been reached. When the mass change between successive readings (~weekly) was generally less than $\pm 0.5\%$, testing was deemed complete and gravimetric water content as a function of suction, $w(h)$, h was determined according to the following equation:

$$w(h) = \frac{W_w(h)}{W_s} \quad (3)$$

where $W_w(h)$ is equal to the weight of water removed during drying after equilibration at suction h , and W_s is the final dry weight of the wafer.

Table 4 Salts used in constant vapor pressure method for moisture retention characteristics.

Salt	Relative Humidity	Suction, cm H₂O
K ₂ SO ₄	0.97	38,293
KNO ₃	0.92	116,653
NaCl	0.75	396,890
KI	0.69	521,158
NaBr	0.58	771,771
MgCl	0.33	1,551,051
LiCl	0.11	3,050,396

$\rho_l = 1000 \text{ kg/m}^3$, $R = 8.3143 \text{ J/mol}^\circ\text{K}$, $T = 296^\circ\text{K}$, $M_v = 0.018 \text{ kg/mol}$
 $1 \text{ Pa} = 1.0197\text{E-}02 \text{ cm H}_2\text{O}$

Effective saturation at suction h , $S_e(h)$, was determined from w according to the following relationship:

$$S_e(h) = \frac{w(h) * \frac{\rho_b}{\rho_w}}{\theta_s - \theta_r} \quad (4)$$

when the moisture is water with a specific gravity of 1.0.

Data ($S_e(h)$, h) from the CVP tests were analyzed to determine the vG curve fitting parameters α and n . Non-linear regression analysis was performed using the Microsoft Excel Solver add-in to fit the vG curve equation 1 to measured moisture retention data for the wafers cut from waste monoliths. $S_e(h)$ was calculated using equation (4) where θ_s = porosity (determined independently according to the techniques described above in the Density and Porosity section). θ_r is assumed to equal 0.00 for grout, while h is equal to vapor pressure. The predicted moisture retention curves were based on moisture retention data only; no unsaturated hydraulic conductivity data were available for the samples. The Mualem (1976) retention curve model $m = 1 - 1/n$ was used to estimate curve fitting parameters.

3.1.2.4 Compressive Strength

After curing 28 days, 5cm diameter x 10cm long cylindrical samples were demolded and tested for compressive strength in triplicate using unbonded caps (ASTM, C39/C39M – 15a).

3.1.2.5 Dimensional Stability

Clumps of fibers used as an admix in Mix 1 were observed in grout monoliths by Nichols et al. (2017) during the visual examination of molded samples that had been cut in half. This type of fiber is commonly used in concrete containing aggregate for “slab on grade” applications to prevent shrinkage cracks. The aggregate in concrete mixes breaks up the fiber when it is mixed and maintains separation of the smaller fiber assemblages during mixing. The lack of aggregate in Mix 1 may allow the formation of clumps of fibers of during mixing. ASTM (C490-11) for determining dimensional stability was used to assess the efficacy of fiber in Mix 1.0. Prisms of grout from Mix 1.0 with and without fiber were prepared and measured for dimensional stability. Fresh grout as prepared and placed in 25 by 25 by 285 mm molds (allowed to cure 24 hours in a sealed bag with a moist towelette, Figure 8(a)). After 24 hours, the prisms were removed from molds and submerged in a lime water bath for 28 days. Length of the prisms was periodically measured using a length comparator, Figure 8(b). Prisms without fiber were tested due to a termination in funding.

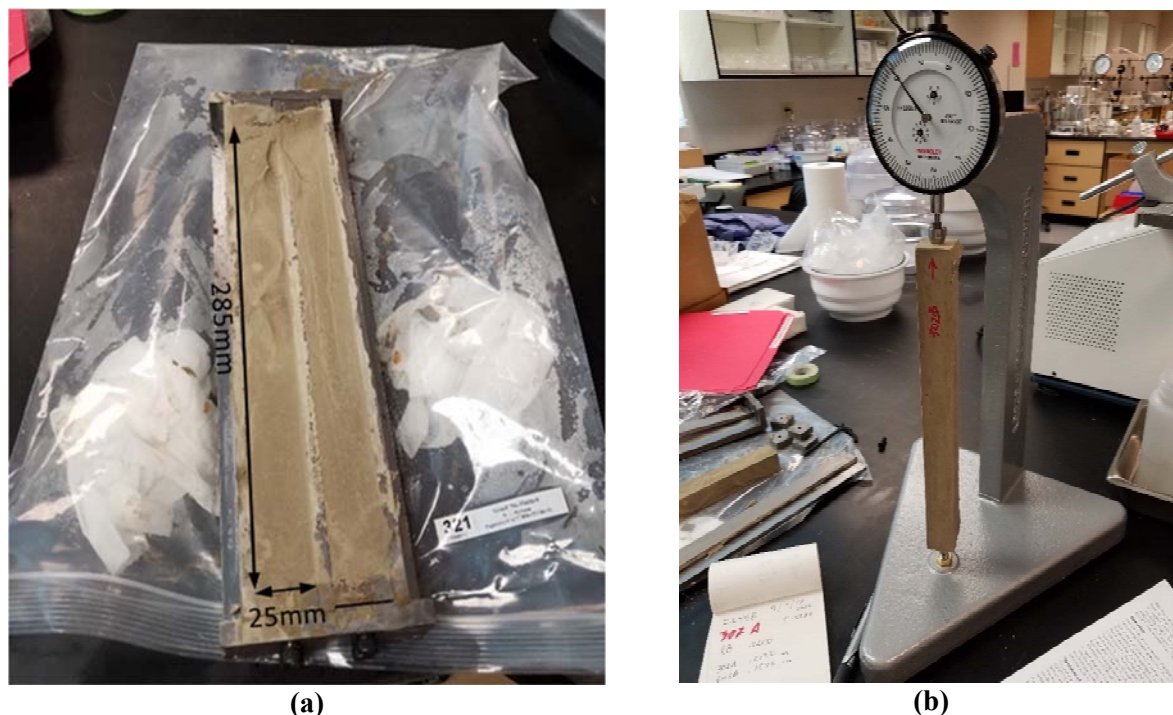


Figure 8 Grout prisms for dimensional stability testing (a) prism in curing mold, (b) comparator for measuring prism length.

3.2 Radionuclide Retention in Grout

Grout batches were prepared using ASTM (C150-18) Type I-II cement (OPC), BFS, Class F fly ash, sand (SD), admix BASF Pozzoloth 80 and BASF Master Fiber M100 single monofilament polypropylene fibers from samples provided by American Rock Products, Lafarge Northwest, and BASF. The formulations used to study ^{99}Tc and I retention in grout are presented in Table 5. Only Mix 1.0 contains admix BASF Pozzoloth 80 and BASF Master Fiber M100. The elemental composition of the cementitious materials used in this study was determined using x-ray fluorescence, results are presented in Table 2. Grout monoliths were prepared using the same method described in section 3.1 Grout Stabilized sRF Resin except that no sRF resin was added.

Table 5 Formulation of mixes used to study radionuclide retention in grout.

Mix	H ₂ O:CM (w/w)	FA/OPC/BFS (w/w)
1.0	0.29	75/25/0
5.0	0.45	20/5/75
13.0	0.45	45/10/45

A solution prepared from a 2:1 (wt/wt) water:grout suspension was used as leachate in partitioning coefficient experiments. To prepare the solution, grout (Mix 1.0, Mix 5.0, or Mix 13.0) was ground to pass a 2mm sieve mixed with water and equilibrated for 3 days on a platform shaker. The solid and liquid phases were separated by settling, followed by 0.45 μm filtration. The leachate was used as the aqueous phase in the K_d batch tests.

The aqueous phase of the 2:1 suspensions used to simulate grout porewater was analyzed by standard methods (EPA, 2009), including pH, dissolved inorganic- and organic-carbon by the oxidation to CO₂ and detection by an infrared detector, ion chromatography (IC), inductively coupled plasma atomic emission (ICP-AES), and inductively couple plasma mass spectroscopy (ICP-MS). Oxidation-reduction potential was measured using platinum electrodes (Ag/AgCl reference electrode) and the results were reported as standard hydrogen electrode values. Dissolved organic carbon was determined by the Shimadzu TOC-L Laboratory Total Organic Carbon Analyzer (Shimadzu, Kyoto Japan). A Carbon-Hydrogen-Nitrogen (CHN) analyzer and a loss-on-ignition (550 °C) standard method were used to quantify organic carbon in the solid phase. All aqueous chemistry measurements were conducted in duplicate

3.2.1 ⁹⁹Tc Partitioning Coefficients

Adsorption partition coefficients (K_d) measurements were conducted following standard methods ASTM (C1733-10), a brief description of the method follows. Grout solids were first washed in two steps with grout leachate solution prior to K_d testing with ⁹⁹Tc (99TcO₄⁻ in a 0.001 M KOH solution) spiked leachate. To wash the grout 0.5g grout and 5 mL of appropriate grout leachate solution were added to a 15-mL centrifuge tube and put on a platform shaker for 15 minutes, and then the phases were separated. A second wash was conducted after 24 hours. Again, the leachate was removed by centrifugation and the washed solids were saved for subsequent K_d measurements. The mass of water remaining in the tube after the last wash was gravimetrically determined and accounted for when estimating K_d values. 12.5 mL of grout leachate amended with 204 dpm/mL ⁹⁹Tc was added to the washed grout samples. In addition to the 25:1 grout suspension samples, two types of liquid controls were prepared. The controls consisted of (1) a blank comprised of filtered leachate and spike, and (2) a reference comprised of distilled water and spike. The reference control provided a measure of whether radionuclides sorbed to labware (e.g., glassware, filters) during the equilibration and phase separation steps. The blank control provided a measure of whether amendments the background solution promoted precipitation of the radionuclide spike or whether the background solution (unknowingly) contained the radionuclide. All tests were conducted in triplicate.

The suspensions were put on a platform shaker for 2 weeks and then the phases were separated by settling, followed by 0.45-μm filtration. Aqueous Tc-99 was measured by liquid scintillation counting and the K_d values were calculated by difference as described in the standard method ASTM (C1733-10):

$$K_d \equiv \frac{c_s}{c} \quad (5)$$

$$c_s = \frac{(V * c_0) - (V * c_f)}{M_s} \text{ and } c \equiv c_f \quad (6)$$

where: c_s = constituent concentration in solid phase

c_0 = initial concentration in solution

c_f = final concentration in solution

V = total volume of liquid

M_s = dry mass of solid

3.2.2 Iodine Partition Coefficient

Mix 1.0 and 13.0 were used in the measurement of iodine adsorption and desorption K_d . The general procedure for making these grout samples was presented earlier in section 3.2.1. Adsorption tests were conducted by contacting grout with a solution (simulated pore water) spiked with either I⁻, IO₃⁻, or 4-iodoaniline (org-I) as stable ¹²⁷I. The 4-iodoaniline form of iodine was selected to represent organo-iodine and is only one of potentially dozens of forms of organo-iodine in Hanford waste. Desorption tests were conducted using <0.1 mm grout samples prepared with an iodine spiked water.

3.2.2.1 Iodine Desorption

Grout monoliths were made using Mix 1.0 and Mix 13.0 and an iodine solution for the desorption study. The $I^-/IO_3^-/org-I$ solution contained of 190 μM of iodine (stable ^{127}I) as either I^- (from KI), IO_3^- (from KIO_3) or org-I (from 4-iodoaniline) and water. Grouts were prepared by adding dry mix to a beaker containing iodine solution that was being stirred by an overhead mixer. Ingredients were mixed for five minutes and the mixer speed was adjusted to maintain a vortex in the grout. Occasionally the mixer was stopped to “burp” the grout and remove air pockets. Once the mixing was complete the grout was decanted into molds to cure. The Mix 13 (containing 45 wt-% slag) monoliths were cured in a moist vacuum-sealed bag placed in an inert glovebox (95% $N_2/5\% H_2$) and the Mix 1 (containing no slag) monoliths were also cured in a moist vacuum-sealed bag, but on the bench top. After 3-months of curing, subsamples of the monolith were ground with a mortar and pestle to pass through a 0.1 mm sieve either on the benchtop (Mix 1) or in an inert glove box (Mix 13).

Desorption experiments were conducted with Mix 1.0 and Mix 13.0 grout samples that were prepared with 19 mmol/L iodine as either I^- , IO_3^- , or 4-iodoaniline. The term desorption is used here in a generic manner, devoid of grout release mechanism and is intended to be used in a similar manner as the term “sorption” is used to describe solid phase uptake processes. Because the iodine was initially associated with the ground grout samples, it is possible that the iodine was released into the aqueous phase as a result of leaching from the particle porewater, desorbing from particle surfaces, or dissolving from solid iodine phases. Because of differences in the solution:CM ratios between the Mix 1 and Mix 13, the final iodine loading into the monoliths was 0.43 and 0.59 $\mu mol/kg$, respectively. The iodine-amended grout samples were ground to pass a 2-mm sieve and then used to create 1:5 solid:liquid ratio suspension. The 1:5 solid: liquid ratio was selected to ease iodine speciation detection. A low ratio was needed to ensure that sufficient iodine was desorbed into the aqueous phase to permit analytical detection, while at the same time, a sufficient aqueous volume was needed after phase separation to permit making the three iodine species measurements per sample (iodide, total inorganic iodine (used to estimate iodate), and total iodine (used to estimate org-I)). A grout leachate was prepared as described in Section 3.2 and the suspensions were placed on a platform shaker. Aqueous samples were collected by passing the samples through 0.1- μm membrane after 1, 3, 7, 14, 21, and 28 days of contact and then analyzed for iodine speciation.

3.2.2.2 Iodine Adsorption

Adsorption experiments were conducted in duplicate with the ground Mix 13.0 samples in an inert glovebox and the Mix 1.0 samples on the benchtop. The solid to aqueous phase ratio was 5 g to 25 mL and the initial amended aqueous iodine concentration was 20 μM (2.58 mg/L; 8000 cpm ^{125}I) of iodine made from $^{125}I/^{127}I$ as either I^- or IO_3^- . The ^{125}I was added as a tracer to account for background ^{127}I and to improve detection limits. The aqueous phase was a grout-leachate created with either Mix 1.0 or Mix 13.0 by mixing a 1:2 grout:water suspension for 3 days and then passing it through a 0.1 μm filter. The solids were ground to pass a 1-mm sieve. The suspension was placed on a platform shaker for 14 days, pH and Eh were measured, the aqueous phase was recovered by centrifuging and filtering (0.1 μm), and then the aqueous phase was analyzed for iodine speciation.

3.2.2.3 Iodine Speciation

Iodine speciation was determined according to procedures reported in Zhang et al. (2010a). Briefly, iodide concentrations were quantified using gas chromatography-mass spectrometry (GC-MS) after derivatization to 4-iodo-N,N-dimethylaniline followed by solvent extraction with cyclohexane. Iodate concentrations were quantified by measuring the difference of iodide concentrations in the solution before and after reduction by $Na_2S_2O_5$. Total iodine, including inorganic and organic iodine, was measured after conversion to iodate by combustion at 900 °C, followed by reduction to iodide as described above. Organo-iodine was calculated as the difference between the total iodine and total inorganic iodine (iodide and iodate). All

analyses were conducted in glass vials, and if samples had to be stored prior to analysis (<1 week), they were placed in 4 °C in opaque containers. Fresh standard solutions and blanks were prepared each day.

The aqueous phase of the 1:2 Mix 1.0 and Mix 13.0 leachates used to simulate background grout porewater were also analyzed by standard methods (EPA, 2009), including pH, dissolved inorganic- and organic-carbon by oxidation to CO₂ and detection by an infrared detector, ion chromatography (IC), inductively coupled plasma atomic emission (ICP-AES), and inductively couple plasma mass spectroscopy (ICP-MS). Oxidation-reduction potential was measured using platinum electrodes (Ag/AgCl reference electrode) and the results were reported as standard hydrogen electrode (SHE) values (the ORP measurements were converted to SHE based on solution temperature (230 mV at 25 °C). Dissolved organic carbon was determined by the Shimadzu TOC-L Laboratory Total Organic Carbon Analyzer (Shimadzu, Kyoto Japan). A CHN analyzer and a loss-on-ignition (550 °C) standard method were used to quantify organic carbon in the solid phase. All aqueous chemistry measurements were conducted in duplicate.

4.0 Results

4.1 Grout Stabilized sRF Resin

4.1.1 *Incorporation of sRF Resin into Grout*

A trial waste form was prepared with CM Mix 1 and with 0.2 v/v drained sRF resin to test the mixing method and confirm incorporation of sRF resin into grout. Waste forms containing 0.1 and 0.3 v/v sRF resin were prepared following preparation and visual inspection the trial waste form with 0.2 v/v sRF resin. sRF resin monoliths were removed from their molds after curing and used for macroscopic photography, three-dimensional micro computed tomography (3d-μCT) and scanning electron microscopy with energy-dispersive x-ray spectroscopy (SEM-EDX). Samples were prepared for direct visual inspection by cutting a monolith lengthwise using a wet band saw. Samples were prepared for 3d-μCT by oven drying at 105°C. Figure 9(a) shows a photograph of a split sample originally used to assess curing and (b) is a slice from a 3d-μCT scan of a 5cm diameter x 10cm long monolith from the same test batch. Distribution of sRF resin particles in the cementitious waste form was determined by direct visual inspection and using 3d-μCT. Both images in Figure 9 show the sRF resin is homogeneously distributed in the grout. Gray specks in the μCT image are the resin and the black swirl is air entrained in a clump of fibers. Fibers shredded by hand prior to mixing formed a clump entraining air in the grout. The clump formed due to a lack of aggregate in the mix which serves to shred and disperse the fibers. Aggregate is commonly used in concrete but is not used in the baseline mix (Mix 1) which does contain fiber. The formulations for Mix 5 and Mix 13 do not contain fiber.

SEM revealed the presence of small cracks in the immediate vicinity of the sRF resin - cement paste interface, Figure 10 producing pores that are much larger than those found in the bulk paste. These cracks may be due to reduced strength of the cement paste near the sRF resin. Anhydrous cement grains may be more loosely packed in the immediate vicinity of sRF resin particles resulting in higher porosity and H₂O:CM similar to that reported by Olliver et al. (1995). A microstructure of cement paste in the vicinity of aggregate with properties different than the bulk cement paste has been studied by several researchers including Olliver et al. (1995) and Scrivener and Nemati (1995). This region around the aggregate is referred to as the interfacial transition zone (ITZ) and has been found to have mechanical and transport properties different than the bulk cement paste. Olliver et al. (1995) reported that the ITZ has a lower microhardness and abrasion resistance than the bulk cement paste. The sRF may be serving a role producing the alteration zone similar to aggregate in concrete producing an ITZ.

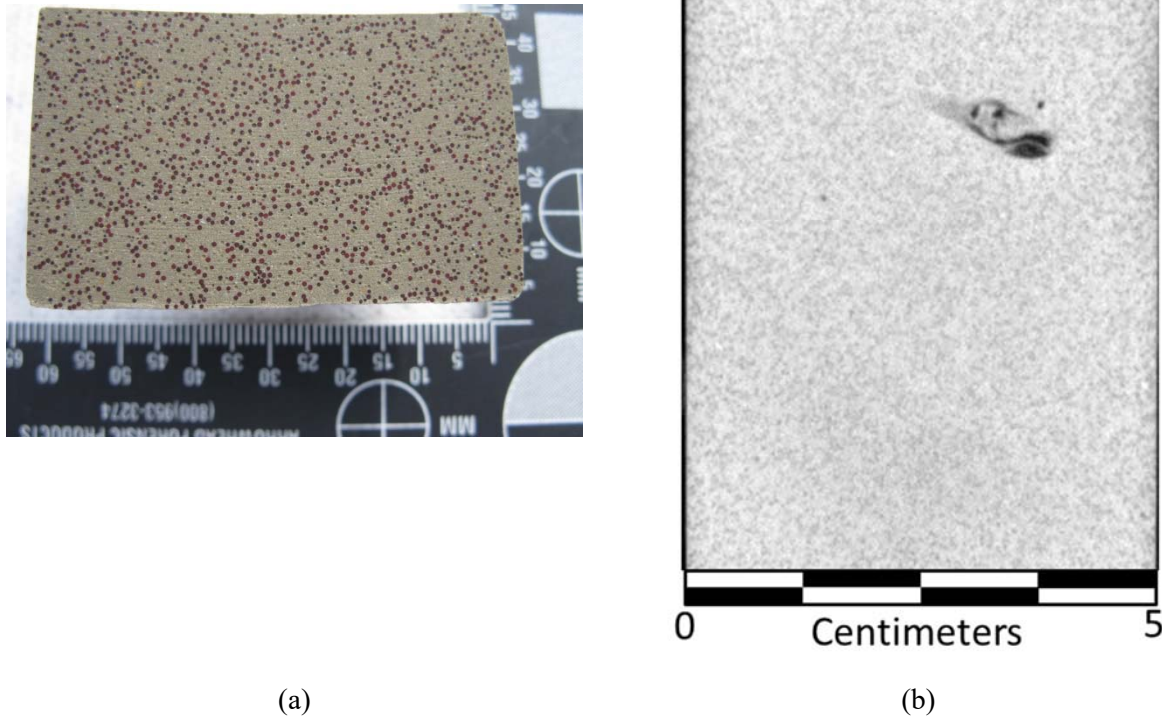
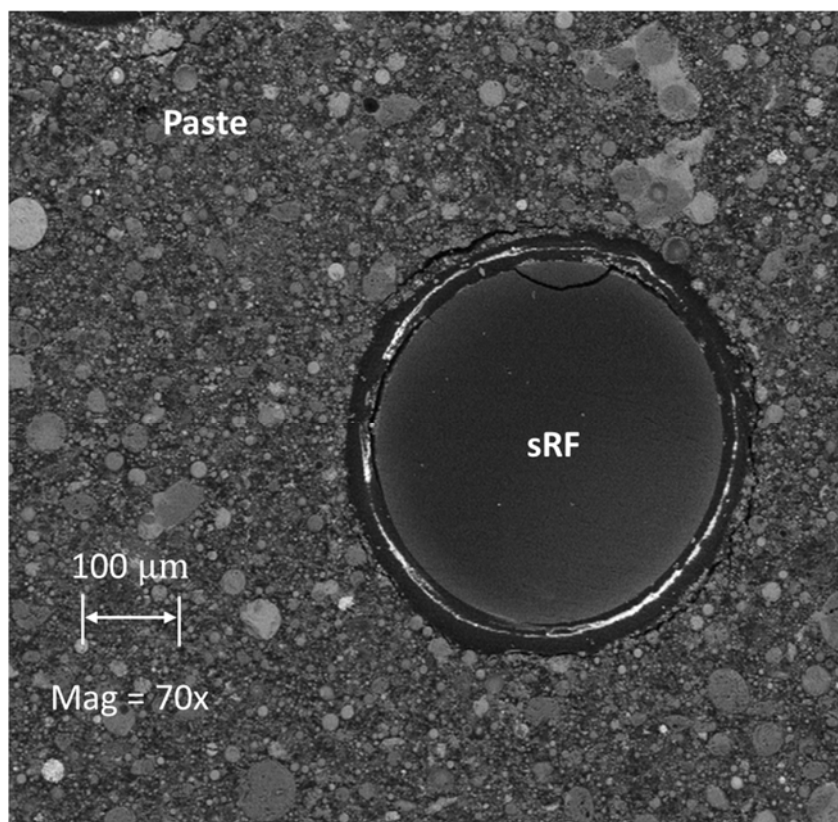
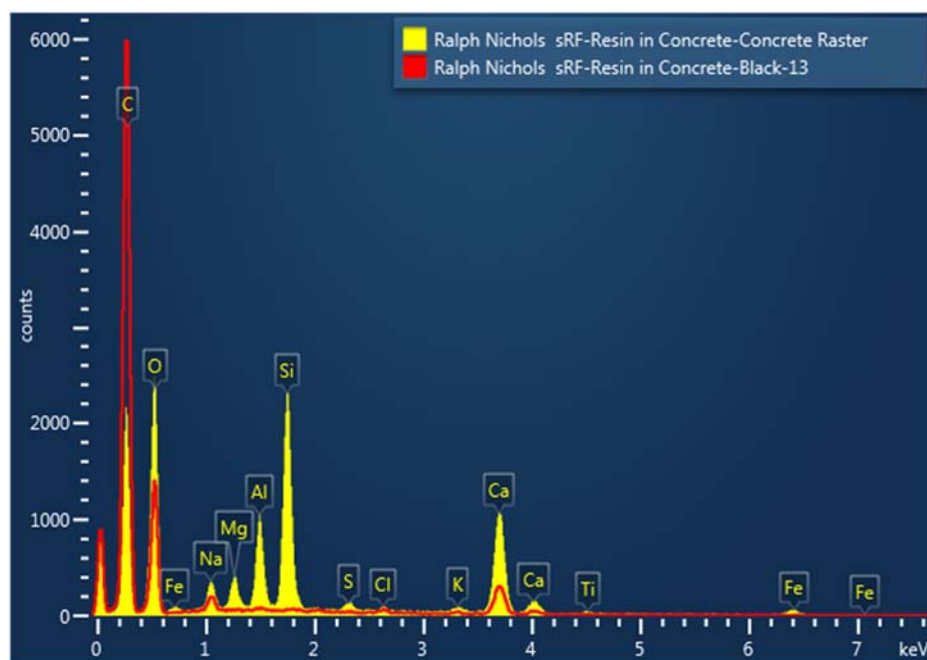


Figure 9 Simulated waste form with 0.2 v/v sRF resin loading Mix 1.2 grout, (a) macroscopic photograph and (b) μ CT slice.

As previously mentioned small cracks were observed around sRF resin particles. The large porosity introduced by the cracks around individual sRF particles is not interconnected and drainage and hydraulic conductivity will be controlled by the bulk paste in between sRF particles. Winslow and Liu (1990) and Synder et al. (1992) studied the pore networks of mortars using mercury intrusion porosimetry and found that above a threshold sand content of 0.45 v/v there was an increase in the volume intruded at pressures corresponding to pore neck sizes between 0.1 μm and 10 μm and concluded that the ITZ around the sand grains had become interconnected or percolated. Based on these results, it was concluded that sRF resin loading in excess of 0.45 v/v may cause percolation resulting in increased drainage at lower suctions due to interconnection of large pores around sRF particles. This would also result in an increase in saturated hydraulic conductivity. If the affected zone around sRF particles is larger, percolation may result at lower sRF loading.



(a)



(b)

Figure 10 Scanning electron micrograph (a) and energy dispersive x-ray spectra (b) of sRF resin particle stabilized in grout where yellow is paste and red is sRF particle sRF resin stabilized in grout.

4.1.2 Formulation Refinement

Preparation of simulated waste forms required adjustments to the initial planned H₂O/CM ratio to get mixes that met the grout flowability criteria of ≥ 120 mm used in the grout study for SSW conducted by Nichols et al. (2017), Table 6. An additional criterion of no bleed at 72 hours was set in coordination with the conceptual model for solidifying drained sRF resin. Drained sRF resin contained more water than was originally anticipated resulting in thin grouts that did not meet the no bleed after 72 hours requirement. Specifically, Mix 5.3 and Mix 13.3 were both soft to the touch and had excessive ($>25\%$ v/v) bleed. The H₂O:CM was adjusted to accommodate the residual water in drained sRF resin. Mix 1 was prepared as originally planned. The final H₂O:CM used in the mixes are listed in Table 6. The amount of water added to the mix may need to be adjusted depending on water content of the drained SRF being stabilized.

Table 6 Mixes used in simulated waste forms.

Mix	Planned H ₂ O:CM (w/w)	FA/OPC/BFS (w/w)	Final H ₂ O:CM (w/w)	Actual sRF, v/v	Actual sRF, w/w	Comment
1.1	0.29	75/25/0	0.39	0.11	0.05	Prepared as intended
1.2	0.29	75/25/0	n/a	0.20	n/a	Prepared as intended
1.3	0.29	75/25/0	0.65	0.31	0.15	Prepared as intended
5.1	0.45	20/5/75	0.57	0.10	0.05	Prepared as intended
5.3	0.45	20/5/75	-	-	-	<i>Too wet, abandoned</i>
5.3a	0.10	20/5/75	-	-	-	<i>Too dry, abandoned</i>
5.3b	0.25	20/5/75	0.58	0.31	0.14	Prepared as intended
13.1	0.45	45/10/45	0.56	0.09	0.05	Prepared as intended
13.3	0.45	45/10/45	-	-	-	<i>Too wet, abandoned</i>
13.3a	0.10	45/10/45	-	-	-	<i>Too dry, abandoned</i>
13.3b	0.25	45/10/45	0.56	0.30	0.14	Prepared as intended

Note: $v/v = \frac{v_{sRF}}{v_{Total}}$

Figure 11 illustrates the composition of the final waste forms containing sRF resin and compares them to the mixes analyzed in Flach et al. (2016a). Mixes in Flach et al. (2016a) contained aggregate (sand and/or gravel) while mixes in this study particles of sRF resin.

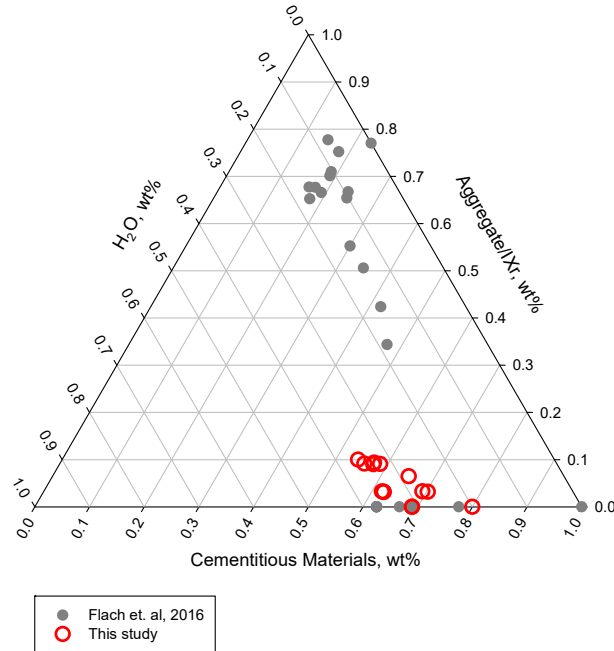


Figure 11 Ternary diagram showing mix designs used in this study.

X-ray fluorescence (XRF), a non-destructive chemical analysis method, was used to determine the composition of the grout matrices produced in this study. XRF results are presented in Table 7.

Table 7 Results from x-ray fluorescence analysis of Mix 1, Mix 5, and Mix 13.

	Mix1	Mix5	Mix13
CaO, wt%	22.5	33.8	27.4
SiO ₂ , wt%	38.2	33.1	35.1
Al ₂ O ₃ , wt%	13.1	13.4	13.7
Fe ₂ O ₃ , wt%	4.5	1.9	3.0
SO ₃ , wt%	0.8	2.1	1.1
MgO, wt%	3.7	4.9	4.5
K ₂ O, wt%	1.1	0.6	0.9
TiO ₂ , wt%	0.6	0.6	0.7
Na ₂ O, wt%	2.2	0.9	1.8
SrO, wt%	0.2	0.1	0.2
P ₂ O ₅ , wt%	0.2	0.1	0.1
Mn ₂ O ₃ , wt%	0.1	0.2	0.1
LoI, wt%	12.8	8.3	11.4

Note: LoI = lost on ignition @ 1000°C

4.1.3 Drained sRF Resin Water Content

The method used to drain sRF resin was repeatable and produced batches of drained sRF resin with similar gravimetric water content, Table 8. This made preparing additional batches easy and improved our

confidence in replicate batches. The drained sRF resin provided by AVANTech, Inc. for gravimetric moisture content determination contained less water than the drained sRF resin used in the tests in this report, Table 9. The amount of residual water in drained sRF resin will need to be considered in sRF resin stabilization grout recipes to create similar flow and other properties related to H₂O:CM.

Table 8 Water content of resin used in final batches.

Mix	Batch ID	sRF H ₂ O, g/g
1.1	1.1 042517	0.66
1.1	1.1 050917	0.69
1.3	1.3 050217	0.67
1.3	1.3 051917	0.68
5.1	5.1 042617	0.69
5.1	5.1 051117	0.68
5.3	5.3b 081017	0.66
5.3	5.3b 070517	0.67
13.1	13.1 042717	0.68
13.3	13.3b 070517	0.68
13.3	13.3b 081017	0.67

Table 9 Water content of resin received from AVANTech.

Sample	sRF H ₂ O, g/g
LAWPS-FS-T9-P2-00375A-101	0.45
LAWPS-FS-T9-P2-00375A-102	0.44
LAWPS-FS-T9-P2-00375A-103	0.45
LAWPS-FS-T9-P2-00375A-104	0.45
LAWPS-FS-T9-P2-00375A-105	0.45
LAWPS-FS-T9-P2-00375A-106	0.45

4.1.4 Fresh Properties

4.1.4.1 Grout Flow

As previously mentioned the grout flow for some of the H₂O:CM had to be adjusted to meet a guide for a flow of ≥ 120 mm. This was accomplished by adjusting the amount of water used to prepare the grout, Table 6. Table 10 shows the grout flow for the final formulations tested.

4.1.4.2 Set

All the final grout formulations used in this study met the set time criteria of <2mm Vicat penetration after 72 hours of curing.

Table 10 Flow properties of grouted sRF resin waste forms.

Mix	H2O:CM (w/w)	FA/OPC/BFS (w/w)	Grout Flow, mm
1.0 ¹	0.29	75/25/0	120
1.1	0.38	75/25/0	149
1.3	0.66	75/25/0	260
5.0 ¹	0.45	20/5/75	128
5.1	0.57	20/5/75	218
5.3b	0.57	20/5/75	144
13.0 ¹	0.45	45/10/45	178
13.1	0.56	45/10/45	246
13.3b	0.68	45/10/45	192

Note: ¹ (Nichols et al., 2017)

4.1.4.3 Bleed

A guideline for bleed of no visible bleed was set based on the current process used for encapsulating debris for the Hanford 200 West Area Low Level Waste Burial ground trenches as described in section 2.0 Background of this report. Drained sRF resin had more residual water than was anticipated based on the flow of the same CM mixes without sRF resin reported in Nichols et al. (2017). This resulted in some grouts that were very wet and had excessive free water, >25 % v/v after 72 hours. All of the of the grout formulations that met the guide for flow had no free water after 72 hours and thus met the bleed guideline. This was accomplished by adjusting the amount of free water added to the grout. Only Mix 5.3 and 13.3 had to be adjusted, Table 6.

4.1.4.4 Heat of Hydration

The reaction of water with cement is exothermic and a considerable amount of heat is generated over an extended period. Fly ash has minimal binding/adhering capacity on its own but in the presence of moisture reacts with lime in cement. Silica in FA reacts with the calcium and hydroxyl ions in the fluid grout to form calcium tri-silicate (replacing the Portlandite) which has very low solubility. This reaction is sensitive to heat and therefore heat produced during the reaction between water and cement will increase the chemical activity of the fly ash. Table 11 contains the total heat evolved at 72 hours, time to maximum heat flow, and maximum heat flow for the simulated waste forms and for plain grout reported in Nichols et al. (2017) for comparison.

The time to maximum hydration heat flux was less than 24 hours for all the mixes as expected. Increased sRF resin loading decreased the maximum heat flow and total heat evolved for each of the waste forms. This decrease is due to relative decrease of CM in a given volume of stabilized sRF resin waste form. Klemczak and Batog (2016) studied the heat of hydration with low OPC content and found that replacement of OPC with varying amounts of FA and BFS reduced both maximum heat flow and total heat evolved relative to OPC. The low OPC content of the CM mixes in this study reduced the maximum heat flow for each of the mixes reducing the potential for heat buildup in waste forms which can cause cracking and lead to increased permeability.

Table 11 Heat of Hydration results for mixes prepared.

Mix	H ₂ O:CM (w/w)	FA/OPC/BFS (w/w)	Total Heat Evolved At 72 hr (J/g)	Time to Maximum Heat Flow (hh:mm)	Maximum Heat Flow (μW/g)
1.0 ¹	0.29	75/25/0	130.09	15:49	1394
1.1	0.38	75/25/0	20.19	11:40	925
1.3	0.65	75/25/0	4.86	14:00	529
5.0 ¹	0.45	20/5/75	32.99	17:49	1358
5.1	0.57	20/5/75	11.98	9:08	437
5.3b	0.58	20/5/75	3.55	10:58	126
13.0 ¹	0.45	45/10/45	50.76	20:43	1513
13.1	0.56	45/10/45	-	-	-
13.3b	0.56	45/10/45	2.07	9:04	230
Klemczak and Batog (2016) ²	0.5	0/100/0	269.1	~10:00	2583

Note: ¹ (Nichols et al., 2017), ² Klemczak and Batog (2016) conducted isothermal test @ 20°C compared to 25° used in this study

4.1.5 Cured Properties.

4.1.5.1 Hydraulic Conductivity

Saturated hydraulic conductivity was determined on six simulated waste forms containing sRF resin. The results are consistent with results from a previous study of grouts for encapsulation and solidification SSW conducted by Nichols et al. (2017). The SSW data package for the IDF PA (Flach et al., 2016a) recommended a log-normally distributed probability distribution function (PDF) for K_{sat} of stabilized SSW. Figure 12 compares the results from this study with the PDF proposed by Flach et al. (2016a). The result for sample for Mix 13.1 was duplicated under different test conditions and replicated in a different test cell on the FWP.

4.1.5.2 Density and Porosity

Simulated waste forms containing sRF resin had densities that are lower than the density of the grout itself (1.30 – 1.65 g/cc) reported by Nichols et al. (2017). The lower density is due to the inclusion of sRF which has a particle density ~ 0.45 g/cc, mass of dried H+-form resin per mL of settled H+-form resin under water in a 25-mL graduated cylinder, (Brown et al., 2011) and the increased porosity which resulted from the increased H₂O:CM.

Table 12 Cured properties for simulated waste forms.

Mix	Dry BD, g/cm ³	Porosity, v/v	K _{sat} , cm/sec	Compressive Strength, psi
1.0 ¹	1.65	0.35	<4.0E-10 to 3.02E-8	7340
1.1	1.45	0.42	2.88E-08	4720
1.3	1.07	0.55	5.34E-08	1033
5.0 ¹	1.30	0.51	4.97E-9	2581
5.1	1.15	0.58	3.36E-08	n.a.
5.3b	1.19	0.53	<2.50E-10	1701
13.0 ¹	1.34	0.49	1.06E-9 to 1.72E-9	3374
13.1	1.16	0.54	7.87E-07	2154
13.3b	1.15	0.52	2.42E-08	2277

Note: ¹ (Nichols et al., 2017)

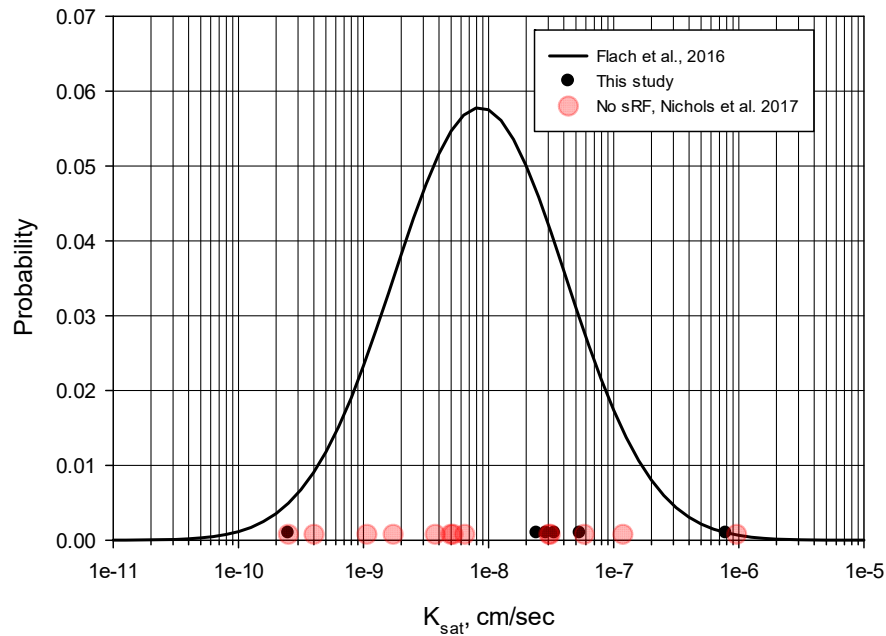


Figure 12 Probability Density Function for materials presented in the initial data package (Flach et. el. 2016) and results for individual grout samples and simulated waste forms containing SRF resin.

4.1.5.3 Moisture Retention

The van Genuchten parameters determined for each of the simulated waste forms are presented in Table 13. There was a good fit between laboratory data and the vG model for water retention, Figure 13. Waste forms which included BFS generally had a higher air entry pressure ($1/\alpha$) than did those without BFS. Waste forms with higher air entry pressure are more difficult to drain as it is more difficult for air to displace water in saturated pores.

Table 13 Van Genuchten curve fitting parameters for simulated waste forms in this study.

Mix	θ_s	θ_r	α, cm^{-1}	n	m
1.1	0.431	0.000	4.30e-6	1.591	0.372
1.3	0.535	0.000	6.20e-6	1.730	0.422
5.1	0.572	0.000	3.97e-6	2.102	0.524
5.3	0.530	0.000	1.45e-6	2.108	0.526
13.1	0.544	0.000	4.40e-6	1.870	0.465
13.3	0.522	0.000	2.86e-6	1.893	0.472
Paste ¹	0.603	0.000	6.47e-6	3.104	0.587
Mortar ¹	0.244	0.148	0.012	1.172	0.143

¹ Table 6-3, Flach et al. (Flach et al., 2016a)

The slope, $\Delta \text{suction} / \Delta \text{saturation}$, of the drainage curve is related to the range of interconnected pore sizes in a material. Images prepared by SEM, Figure 10, show the pore network in a sample of solidified sRF resin obtained from the waste form shown in Figure 9. Material between the individual sRF resin particles appears to be uniform, while pore sizes within the paste, Figure 10, also appear to be uniform. This uniform pore size resulted in a “flat” drainage curve over the saturation range from 0.9 to 0.2, Figure 13.

Simulated waste form WRCs more closely resemble the WRC reported for paste by Flach et al. (2016a) than the WRC reported for mortar, Figure 13. The mortars in Flach et al. (2016a) contained 42% to 84% sand and gravel by weight. This large aggregate content likely resulted in percolation and a larger range of pore sizes which is evident in the steep WRC for mortar compared to the flat WRC for pastes in Figure 13 (a). The low air entry pressure for mortars indicated by drainage at low suction is likely due to the presence of more and interconnected large pores in the mortar. SSW grouts tested in Nichols et al. (2017) have WRCs (green lines in **Figure 13** (b) – (d)) similar to the WRCs for grouted sRF resin waste forms tested in this project, shown as green lines in Figure 13. The similarity between WRCs for grout and sRF resin waste forms further indicates that paste controlled moisture movement in the sRF resin waste forms.

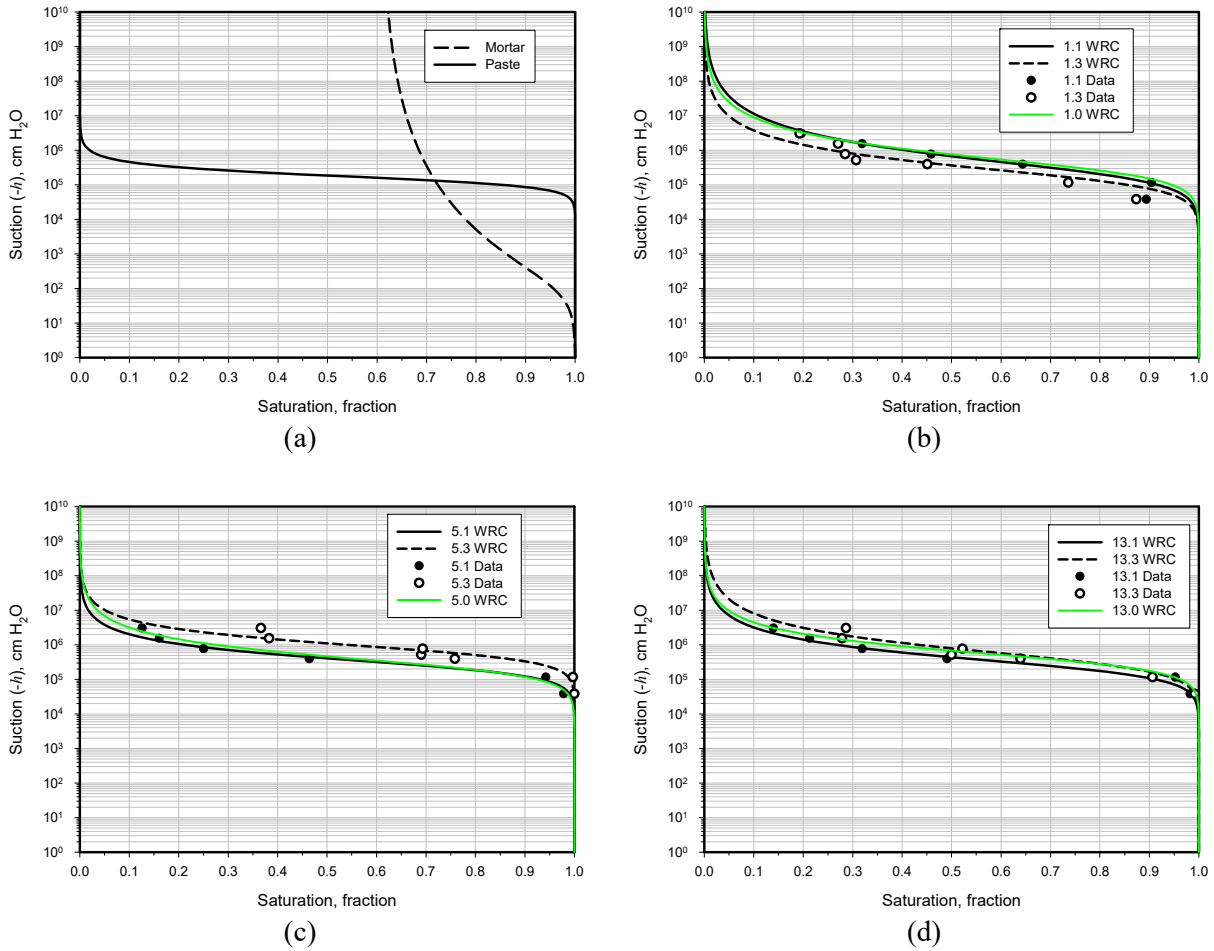


Figure 13 Water desorption curves for simulated waste forms (a) Flach et. al. [4], (b) 1.1 and 1.3, (c) 5.1 and 5.3, (d) 13.1 and 13.3. Note: xx.y = Mix#.sRF loading.

Desorption moisture retention testing (drainage) was initiated on saturated samples and the samples were drained to reach equilibrium with the vapor pressure in sealed containers containing salt solution. Large connected pores drain first, causing hydraulic conductivity to decrease rapidly while capillary forces retain water in small pores. Figure 14 illustrates a capillary tube model for drainage for saturated and drained conditions. A material drained to capillary pressure h_{cl} in Figure 14 (b) will have a lower hydraulic conductivity than the same material saturated shown Figure 14(a) because the large diameter tubes (pores) such as ④ are drained and do not contribute to the hydraulic conductivity. As drainage progresses, capillary forces in small pores connecting large pores will prevent large pores from draining ③ in Figure 14(b) until suction is high enough to drain the small pores. This is commonly referred to as the ink bottle effect (Hillel, 1971). As a result, once drainage begins, small increases in suction result in large decreases in K_{rel} . Figure 15 contains relative hydraulic conductivity curves for the waste forms tested. Note K_{rel} varies 12 orders of magnitude in Figure 15.

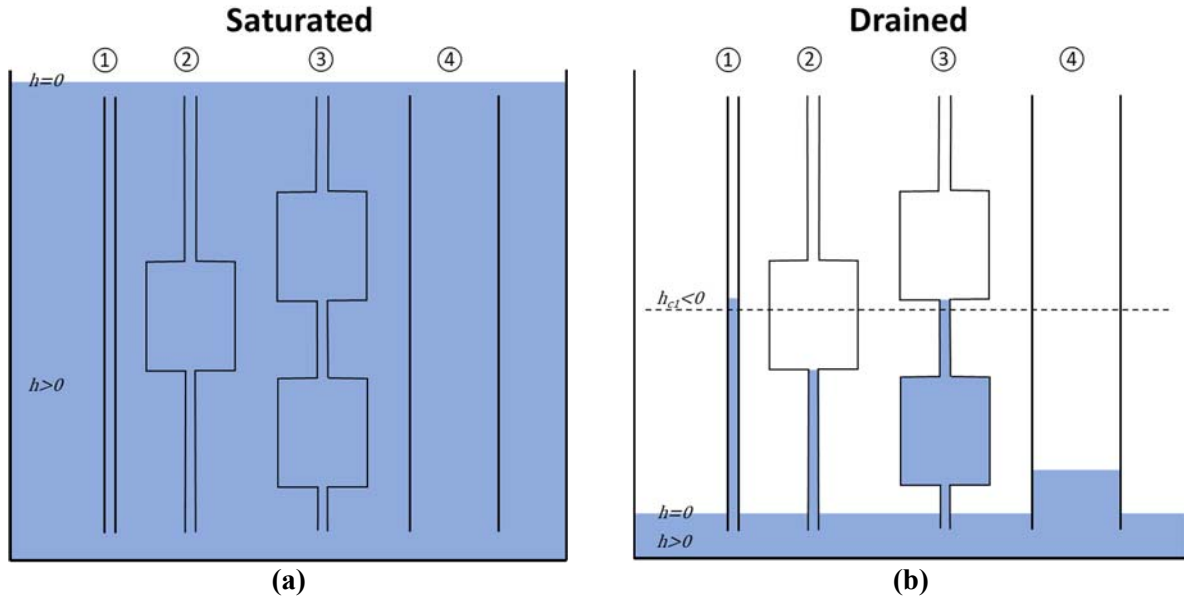


Figure 14 Capillary tube model for pore network in a grouted waste form .

K_{rel} is a function of S_e that is related to pressure head by the van Genuchten equation 7.

$$K_{rel}(S_e) = \frac{K_{S_e}}{K_{sat}} = S_e^L \left[1 - (1 - S_e^{1/m})^m \right]^2 \quad (7)$$

K_{rel}	relative hydraulic conductivity, (cm/sec)/(cm/sec)
K_{sat}	saturated hydraulic conductivity, cm/sec
K_{S_e}	hydraulic conductivity at effective saturation S_e , cm/sec
S_e	effective saturation, $\text{cm}^3_{\text{H}_2\text{O}}/\text{cm}^3_{\text{void}}$
L	empirical pore-connectivity parameter assumed to be 0.5, unitless
m	parameter in the moisture retention equation. unitless

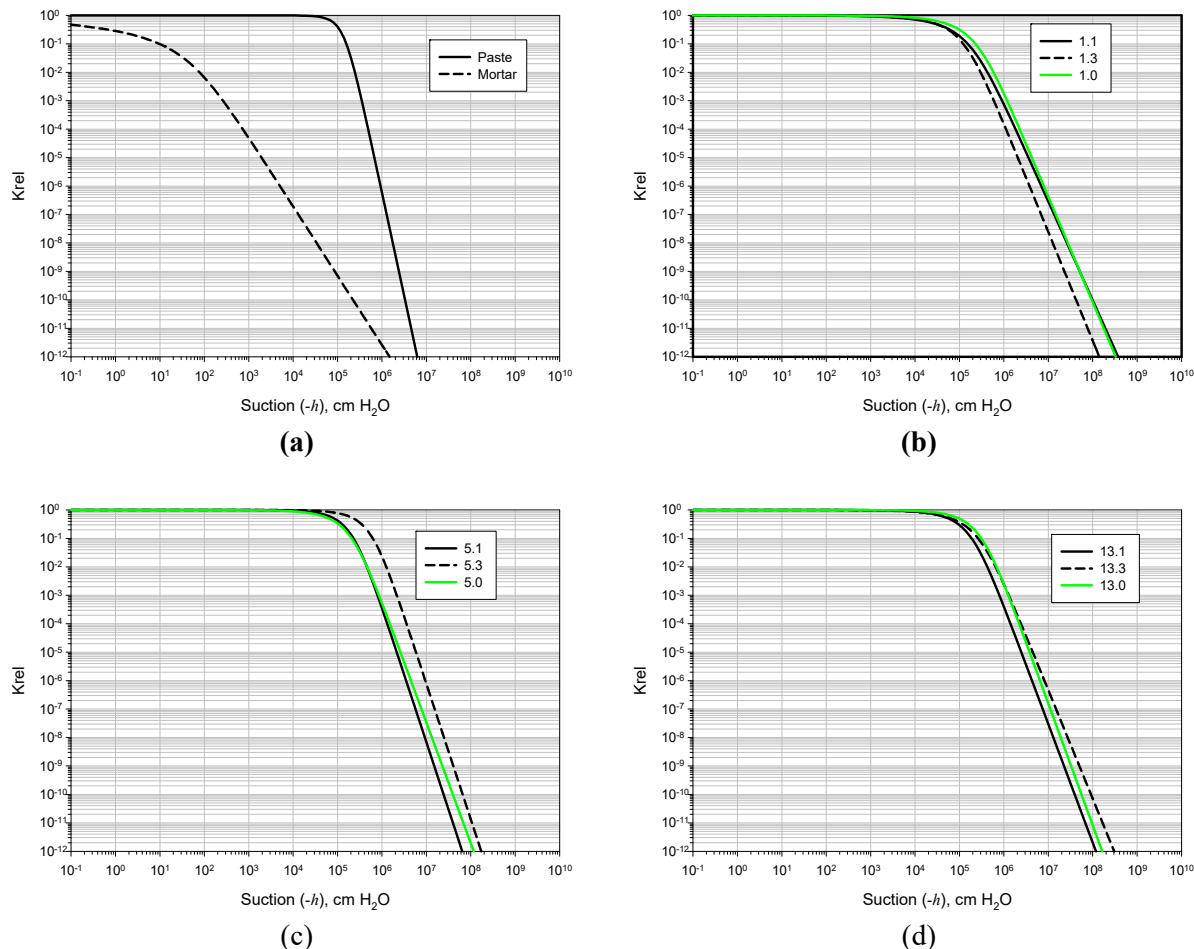


Figure 15 Relative hydraulic conductivity curves for grout sRF resin (a) Flach et al. (2016a), (b) Mix 1, (c) Mix 5, and (d) Mix 13.

4.1.6 Compressive Strength

Grouted sRF resin waste forms had a 28 day compressive strength ranging from 1033 psi to 4720 psi. Addition of sRF resin to grout generally reduced the compressive strength for the CM blends tested compared to grout without sRF resin, Figure 16. Grouted sRF resin had higher compressive strength than Kay et al. (2017) reported for cation resins grouted (36 wt percent) in a 9:1 BFS:OPC blend of 5.2 MPa (754 psi). All of the waste forms tested had compressive strength above the minimum strength of 500 psi after curing for a minimum of 28 days recommended by the U. S. Nuclear Regulatory Commission (NRC, 1991) All mixes with sRF resin achieved sufficient compressive strength for consideration in the use of solidification of SSW followed by subsequent land disposal assuming typical compressive strength requirements for similar applications.

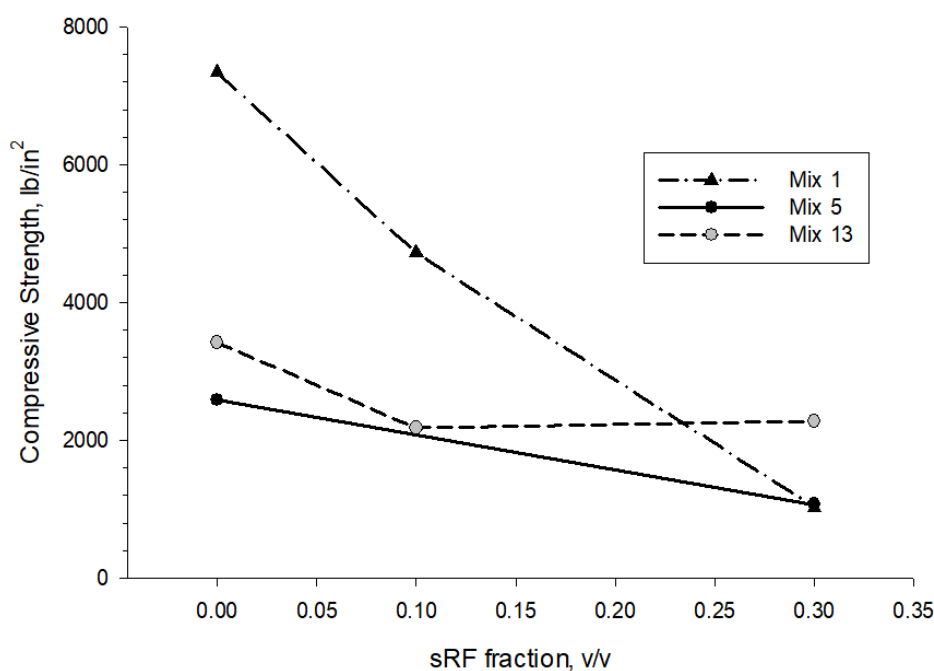


Figure 16 Compressive strength of grouted waste forms with increasing amounts of sRF resin.

4.1.7 Dimensional Stability

Dimensional stability testing was not completed due to a termination of funding. Testing of Mix 1 samples was stopped prior to completion and no prisms containing Mix 1 without fiber were prepared.

4.2 Radionuclide Retention in Grout

Adsorption and desorption experiments were conducted to assess retention of ^{99}Tc and iodine in grouts made from Mix 1.0, Mix 5.0, and 13.0. Mix 5.0 and 13.0 contain BFS to produce reducing grouts while Mix 1 does not contain any BFS and is an oxidizing grout. Reducing grouts are preferred for the retention of ^{99}Tc because it promotes the chemical reduction of Tc from the mobile TcO_4^- form to the appreciably less soluble Tc^{+4} form. Grouts used in these experiments did not contain sRF.

The leaching solution used in these studies was the leachate from a 2:1 liquid:solid suspension Table 14. This grout leachate was designed to approximate the grout porewater. Previously, $\text{Ca}(\text{OH})_2$ and CaCO_3 saturated solutions were used to measure K_d values ((Cantrell et al., 2016); (Kaplan, 2009); (Kaplan et al., 2008); (Serne et al., 2015); (Um et al., 2013); (Um and Serne, 2005); (Um et al., 2011)). While this is convenient, it may not include some potentially important dissolved constituents, especially those that may be important for cation or anion exchange. For example SO_4^{2-} is an especially efficient competitive exchange anion for sediment- or resin-bound TcO_4^- ((Kaplan, 2016); (Williams and Carbone, 2015)). The grout leachate solution used in this study included all the salts comprising porewater (including K, Na, and SO_4^{2-}), not just Ca^{2+} , OH^- and CO_3^{2-} . Furthermore, based on thermodynamic considerations, these additional ions would be expected to impact sorption/desorption processes and pH and Eh levels. The pH levels did not change greatly between the three grout leachate solutions, Table 14, whereas the Eh changed inversely with the percent slag in the grout formulation. The general higher cation (K and Na) and anion (SO_4^{2-}) concentrations in Mix 1.0 can be attributed to the greater amount of cement used in the mix, Table 14.

Table 14 Aqueous chemistry of leaching solution and leachate.

Mix	pH	Eh (mV) ^a	Org-C (ppm)	Ca (ppm)	Fe (ppm)	K (ppm)	Na (ppm)	Si (ppm)	Cl ⁻ (ppm)	NO ₃ ⁻ (ppm)	SO ₄ ²⁻ (ppm)
Leaching Solution (2:1 liquid:solid leachate)											
1.0	12.28	208		8.80	0.06	458.6	1370	10.37	3.47	3.68	330.4
5.0	12.23	18		7.34	0.14	334.2	443	8.08	13.66	1.04	166.1
13.0	12.25	50		5.47	0.31	270.7	546	7.20	13.97	3.16	53.84
14-day equilibration period suspension (25:1 grout-leachate:grout)											
1.0	12.21	196	4.28	8.31	0.10	314.7	1135	13.60	5.44	7.87	323.4
5.0	12.07	-53	-- ^c	46.63	0.39	304.0	410	6.06	13.63	<10.0	54.17
13.0	12.37	77	4.98	38.46	0.48	235.0	512	9.41	23.60	5.02	41.67

^a Eh values were corrected from Ag/AgCl platinum electrode measurements to Standard Hydrogen Electrode (SHE) reference state (corrections varied with solution temperature; e.g., +230 mV at 25 OC).

^b Mn and NO₂⁻ had below detection limit concentrations in all three grout suspensions, <0.010 mg/L and <1.00 mg/L, respectively.

^c Not measured

⁹⁹Tc Uptake by Grout Under Partially Reducing Conditions

An initial study was conducted to determine whether a 14-day contact time was sufficient for Tcaq to come to steady state with the three grout formulations Figure 17; no replicates for this initial study. Tc uptake came to steady state within 4 hours of contact time for Mix 1.0 and 13.0, and 14 days for Mix 5.0. Because Tc K_d values for all three grout mixes converged by day 14, they can be represented by a single steady state K_d value 5.01 ± 0.29 mL/g (n = 3). Importantly, the Tc had non-zero adsorption K_d values.

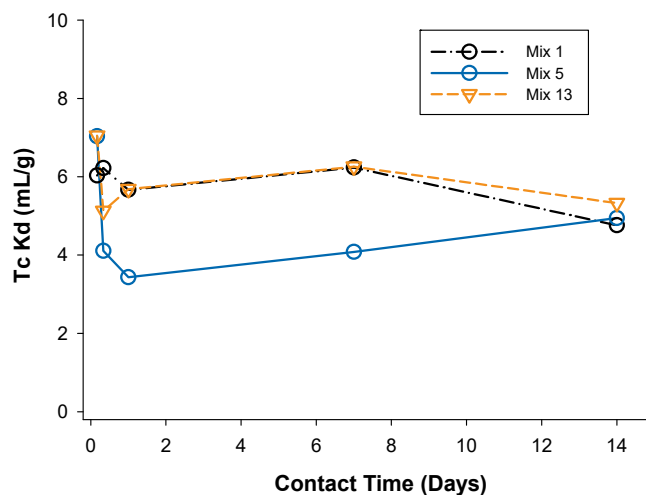


Figure 17 ⁹⁹Tc K_d values measured under benchtop conditions as a function of contact time.

The chemistry of the liquid phase at the end of the 14-day equilibration period deviated somewhat from the chemistry of grout leachate, Table 14. While the Eh of Mix 1.0 and Mix 13.0 did not change greatly, the Eh for Mix 5.0 greatly decreased from 18 mV for the grout leachate to -53 mV for the equilibrium solution, Table 14. These Eh values were apparently not sufficiently low to promote the reduction of all the aqueous Tc(VII) to Tc(IV), as evidenced by the relatively high aqueous Tc concentrations with respect to the $\text{TcO}_2 \cdot x\text{H}_2\text{O}$ solubility concentrations. The system is oxidized with respect to the Tc(IV/VII) oxidation/reduction couple, but is certainly more reduced than at the $\text{O}_2/\text{H}_2\text{O}$ oxidation/reduction couple. As such, the system is a partially reduced system. A grout system that is neither completely oxidized (more specifically, the Eh is poised by Fe(II)/Fe(III) oxidation/reduction couple) or completely reduced (the Eh is poised by the sulfide/sulfate oxidation/reduction couple) may be representative of periods during the transition from the fully reduced to the fully oxidized systems. This type of non-equilibrium is common, if not expected, in geological systems during transition periods, where multiple redox couples act to poise the system (Stumm and Sulzberger, 1992).

The suspension of slag-free grout, Mix 1.0, had an Eh of 196 mV indicating that it was not fully oxygenated, Table 14. To put this into context, vadose zone ground water samples at the Hanford site commonly have Eh values >400 mV (Hartman et al., 2006). This relatively lower Eh value measured in the Mix 1.0 suspensions may be attributed to the reduction capacity of ordinary Portland cement and the fly ash Table 15 (Um et al., 2015). As a point of reference, the reduction potentials for OPC, BFS, and FA used to make Saltstone (Kaplan et al., 2008) is also presented in Table 15. While these reduction potentials were not measured on precisely the materials used in this study, they demonstrate that there is likely some reduction potential not only in the BFS, but also in the fly ash and ordinary Portland cement that may promote the relatively low redox status of the grout leachate, even in the slag-free grout Mix 1.0.

Table 15 Reduction potential of raw solid materials used to make Cast Stone using the of ingredients used in wastefoms at SRS and Hanford.

Solid Phase	Cast Stone^a (meq/kg)	Saltstone^b (meq/kg)
Ordinary Portland Cement	79 ^c	198
Class F Fly Ash	77	299
Blast Furnace Slag	798	819

^a (Um et al., 2015)

^b (Kaplan et al., 2008)

^c Ce(IV)-Fe(II) colorimetric titration method (Angus and Glasser, 1985)

Once it was established through the kinetic study that short-term steady state had been achieved in <14 days, then a second set of ^{99}Tc K_d tests were conducted. The second ^{99}Tc K_d tests used a 25:1 leachate grout ratio and a 14 day equilibration time and were essentially a replicate of the 14 day interval of the kinetic test. The results were like the kinetic test in that: 1) a non-zero K_d value was measured and 2) there was no significant difference between the three grout formulations. The average K_d values for all three grout formulations was 2.79 ± 0.76 mL/g ($n = 6$; K_d value for Mix 1.0 was 2.39 ± 0.50 , for Mix 5.0 was 3.41 ± 0.80 and for Mix 13.0 was 2.59 ± 0.90 mL/g). The cause for the differences between the 14-day ^{99}Tc K_d values from the kinetic test Figure 17 and the equilibrium test Figure 18 is attributed to subsample variability.

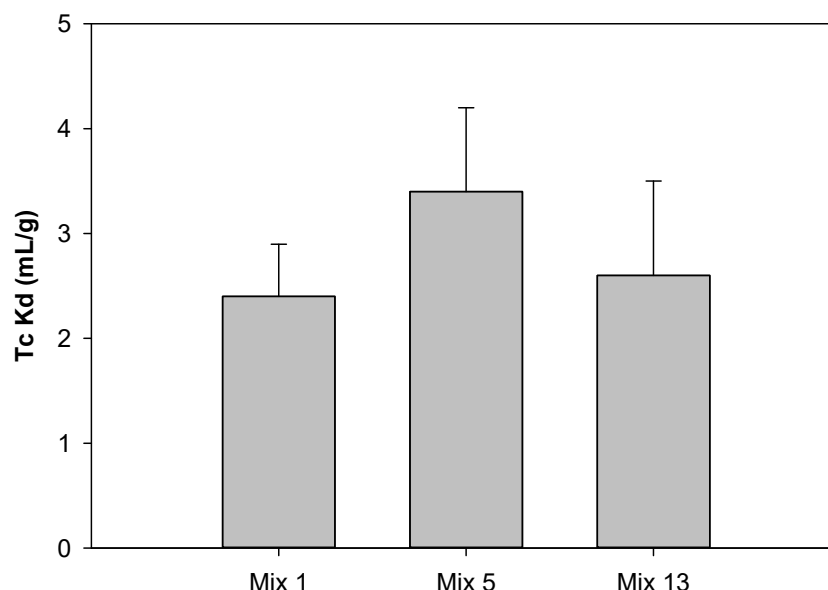


Figure 18 ^{99}Tc K_d values from the equilibrium K_d Test (3 replicates, 14-day equilibrium time, 2:1 grout leachate, 1:5 grout:leachate; measured under benchtop conditions).

4.2.1 Iodine Partition Coefficient

4.2.1.1 Iodine Adsorption

The influence of aqueous iodine speciation on adsorption by grout was measured, Table 16. Irrespective of whether aqueous I^- or IO_3^- was added to the leaching solution, the K_d values were not significantly different ($p > 0.05$; $n = 2$); the overall average for all four measured K_d values was 2.81 ± 0.34 mL/g, Table 16. Also, irrespective of whether I^- or IO_3^- was added to a specific grout suspension, the aqueous iodine speciation did not differ significantly ($p \leq 0.05$; $n = 2$; Table 16), which explains in part why there were no significant differences in the corresponding K_d values. The similarity between speciation distributions suggests that the iodine speciation had reached steady state. However, the presence or absence of slag in the grout formulation greatly alters the steady state iodine speciation. For Mix 1 the percentages of I^- , IO_3^- , and org-I were 40.37%, 14.97%, and 44.67%, respectively. For Mix 13.0, the percentages of I^- , IO_3^- , org-I were 61.94%, 38.06%, and 0%, respectively. One potential explanation for why no org-I formed in the Mix 13.0 system may be that the aqueous conditions do not permit the dissolved iodine to form $\text{I}(0)$ or HIO , which are necessary for iodine to form covalent bonds to organic C.

The 14-day equilibrium solution contained 4.28 and 4.98 mg/L dissolved organic C, in the Mix 1.0 and Mix 13.0 suspensions, respectively Table 14. The organic portion of cementitious material is routinely determined by Loss on Ignition (LoI) data and is an approximate measure of the amount of carbon present (Freeman et al., 1997). Properties of the organic carbon in these materials are not well documented; however, it is commonly measured in concrete and its constituents and is known to impact hardening and durability properties (Kurdowski, 2014). Carbonates, bound water present in hydrated lime or residual clay minerals, sulphides, sulphur, and some iron minerals will decrease the LoI value due to gain in weight because of oxidation. Payá et al. (1998) suggest carbon is, generally, the substance most responsible for ignition loss. Organic C that was identified in Mix 1 and Mix 13, 0.090 wt-% and 0.063 wt-%, respectively was likely derived from carbon LoI from CM used in the grouts, Table 2 and Table 7. Carbon content of Mix 1 and Mix 13 are shown in Table 17

Table 16 Iodine sorption experiments by grout with and without slag in formulation: iodine aqueous speciation and K_d values after 7-day equilibration period.

	Mix 1.0 (Final % of Total Iodine)		Mix 13.0 (Final % of Total Iodine)	
	$I_{(aq)}$ amendment	$IO_3^-_{(aq)}$ amendment	$I_{(aq)}$ amendment	$IO_3^-_{(aq)}$ amendment
$I_{(aq)}$	38.88 ± 0.12^b	41.86 ± 3.17	60.21 ± 0.15	63.67 ± 3.16
$IO_3^-_{(aq)}$	16.43 ± 0.25	13.50 ± 3.17	39.79 ± 0.80	36.33 ± 2.20
Org- $I_{(aq)}$	44.69 ± 2.27	44.64 ± 3.44	0	0
K_d(mL/g)				
I	3.03 ± 0.23	3.06 ± 0.16	2.33 ± 0.10	2.80 ± 0.30

^a Experimental conditions: 5g grout/20 mL liquid (liquid = grout leachate; Table 14, 7-day equilibration in inert glovebox (Grout_{+slag}) or on benchtop (Grout_{-slag}); 20 μ M (2.58 mg/L) of iodine made from $^{125}I/^{127}I$ as either I^- or IO_3^- .

^b All measurements conducted in duplicate and error was calculated by taking into consideration propagation of error.

Table 17 Total iodine, organic and inorganic carbon content of grout from Mix 1.0 and Mix 13.0 after 28 day cure.

mix	total iodine^a (μg/g)	organic C^b (wt-%)	inorganic C^b (wt-%)
Mix 1.0	0.083	0.090	1.127
Mix 13.0	0.177	0.063	0.847

^a Method used was Zhang et al.(Zhang et al., 2010b)

^b Analyzed by CHN analyzer

4.2.1.2 Iodine Desorption

The grout samples used in these desorption experiments were spiked with I^- , IO_3^- , or 4-iodoaniline and then permitted to cure for >3 months. The grout samples were then ground (<0.1-mm sieve) and used to make a 1:5 solid:liquid suspension. Iodine desorbed from the grout into the aqueous phase of the suspension was monitored for 28 days, Figure 19. A ranking of the iodine amendment based on their tendency to leach from the grout were: $I^- \gg 4\text{-iodoaniline} \geq IO_3^-$ Figure 19. For the I^- or IO_3^- amended grout samples, there was no significant difference between the amount of total iodine released from the Mix 1.0 and Mix 13.0 suspensions. For the IO_3^- amended samples, total iodine leached from the Mix 1.0 suspensions were about twice that of the Mix 13 suspensions. Steady state took >28 days to achieve for the Mix 1.0 suspensions and ≤ 14 days for the Mix 13.0 suspensions.

Desorption K_d values using the 28-day leachate concentrations from, Figure 19 and the concentrations measured in the solid phase at the end of the equilibration period, are between 3 and 40 times greater than the uptake K_d values, Table 18. In a manner similar to sorption K_d values, desorption K_d values measured

in this manner are devoid of mechanism. The aqueous iodine may have leached from the pore spaces within the grout particles, desorbed from the surface of particles, or been solubilized from grout solids.

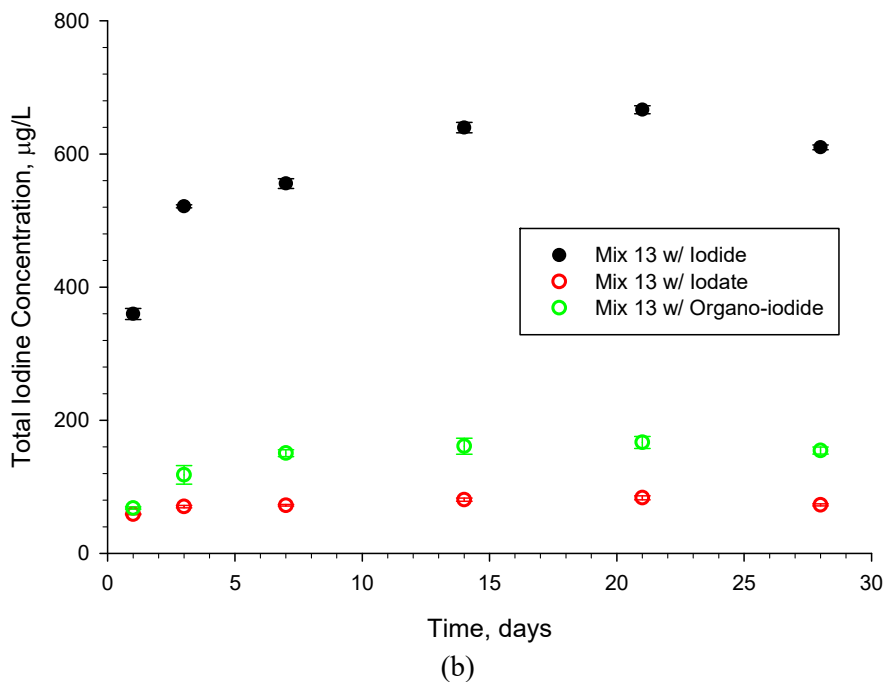
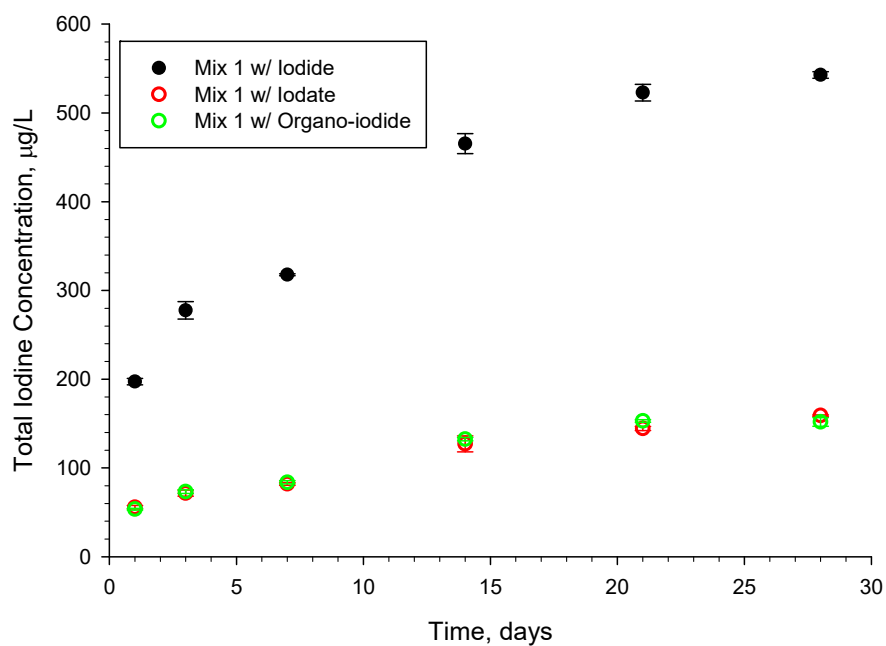


Figure 19 Desorption of iodine from crushed Mix 1.0 and Mix 13.0. Error bars were calculated from duplicate samples and include propagation of analytical error. Error bars may be hidden by symbol.

The finding that desorption K_d values are greater than uptake K_d values, also referred to as sorption hysteresis, has been attributed to several factors, including the need for bound species to break surface-bonds (Ochs et al., 2016). Of the two types of K_d values, the desorption values are more important for risk or reactive transport modelling because they would constitute the rate limiting reaction in the subsurface environment, i.e., the desorption process is slower than the uptake process. Also, while iodine speciation or grout formulation did not have a significant effect on adsorption K_d values (the average adsorption K_d was 2.81 ± 0.34 mL/g) both parameters had significant effects on desorption K_d values, Table 18. Iodide, iodate, and 4-iodoaniline desorption K_d values of Mix 1.0 were significantly less than those from the Mix 13.0 suspensions (Student's t test, $p \leq 0.05$). Furthermore, IO_3^- K_d values were greater than or equal to the 4-iodoaniline K_d values, which were greater than I^- K_d (Tukey's HSD Range Test; ($p \leq 0.05$, $n = 2$), (R Development Core Team, 2017). Iodine K_d for grouts prepared with different iodine species are shown in Figure 20

Table 18 Desorption K_d values (mL/g) as a function of grout formulation and iodine species added to mix prior to curing.

	Iodide	Iodate	4-iodoaniline
Mix 1	$6.14 \pm 0.07^a b^b$	$30.62 \pm 0.17 a$	$32.28 \pm 1.15 a$
Mix 13	$7.50 \pm 0.10 c^*$	$121.78 \pm 9.54 a^*$	$42.07 \pm 2.47 b^*$

^a K_d values (C_{grout}/C_{aq}) were calculated using the 28-day data from Figure 17 (C_{aq}) and the solid concentration at the end of the 28-day equilibration period (C_{grout}). Initially, the total iodine in Grout_{-slag} was 9.077 ± 1.030 $\mu\text{g/g}$ and in Grout_{+slag} was 9.469 ± 1.981 $\mu\text{g/g}$. In a manner similar to sorption K_d values, desorption K_d values measured in this manner are devoid of mechanism. The aqueous iodine may have leached from the pore spaces within the grout particles, desorbed from the surface of particles, or been solubilized from grout solids.

^b Different lowercase letters within a row represent significantly ($p \leq 0.05$, $n = 2$) different values according to Tukey's HSD range test.

* signifies a significant difference ($p \leq 0.05$, $n = 2$) within a column according to Student's t-test.

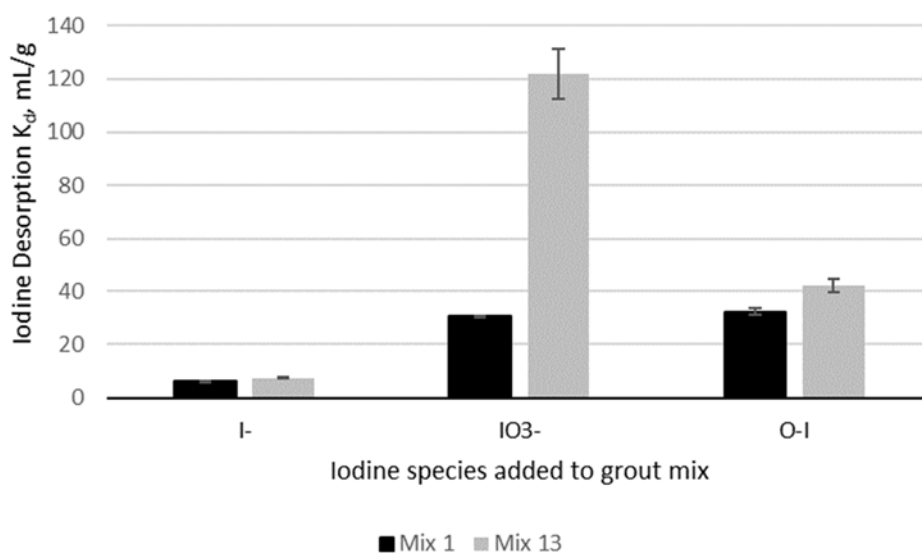


Figure 20 Comparison of desorption K_d for mixes amended with different forms of iodine.

5.0 Conclusions

Drained sRF resin was stabilized in grout consisting of ASTM C-150 Type I-II Cement, Class F fly ash, and blast furnace slag. Three different blends of CM and two different sRF resin loadings were tested. Drained sRF resin contained sufficient residual water that the planned H₂O:CM ratio had to be modified to obtain the desired fresh properties. The maximum heat flow for the formulations containing sRF resin ranged from 126 – 925 μ W/g. The addition of sRF resin reduced the maximum heat flow and total heat evolved during the first 72 hours of curing.

Drained sRF resin was evenly distributed throughout the waste forms. Scanning electron microscopy revealed large pores around individual sRF resin particles. These pores are circumferential to the sRF resin particles and appear to be cracks. These cracks may be due to reduced strength of the cement paste near the sRF resin. A microstructure of cement paste in the vicinity of aggregate with properties different than the bulk cement paste has been studied by several researchers including Olliver et al. (1995) and Scrivener and Nemati (1995). This region around the aggregate is referred to as the interfacial transition zone (ITZ) and has been found to have mechanical and transport properties different than the bulk cement paste. Olliver et al. (1995) reported that the ITZ has a lower microhardness and abrasion resistance than the bulk cement paste. The sRF may be serving a role similar to aggregate in producing an affected zone similar to ITZ on concrete.

All waste-forms had hydraulic properties (saturated hydraulic conductivity and water retention) similar to the grouts they were based on. This indicates that the paste between the individual sRF resin particles is controlling water movement through the waste-forms and is consistent with percolation theory which indicates that particle loadings of at least 45% v/v are required for particle percolation to occur. Particle percolation could result in overlap of the affected zones causing pathways within the waste-form that have higher hydraulic conductivity and more drainage than the bulk paste. Water retention curves for the waste-forms are similar to those recommended for paste in the IDF PA for SSW (Flach et al., 2016a).

Waste forms with a higher sRF resin content had lower compressive strength. However, all of the waste forms tested had compressive strength above the minimum strength of 500 psi after curing for a minimum of 28 days recommended by the U. S. Nuclear Regulatory Commission (NRC, 1991)

All the Tc sorption experiments were completed as originally planned, however some of the iodine sorption experiments were not completed due to budgetary/administrative reasons, but some initial scoping studies related to iodine K_d values were completed. Tc had a non-zero K_d value. Two separate experiments were conducted, a kinetic study and a 14-day equilibrium study, in which Tc K_d values did not differ between grout formulations; the average was 5.01 ± 0.29 mL/g and 2.81 ± 0.34 mL/g, respectively. These measurements were made on the benchtop and the Eh and pH values in the equilibrium solutions suggested that the redox status of the system was partially reducing. A grout system that is neither completely oxidized (more specifically, the Eh is poised by Fe(II)/Fe(III) oxidation/reduction couple) or completely reduced (the Eh is poised by the sulfide/sulfate oxidation/reduction couple) may be representative of periods during the transition from the fully reduced to the fully oxidized systems.

In preliminary studies, adsorption and desorption iodine K_d measurements were conducted. Not surprisingly, the desorption K_d values were 3 to 40 times greater than those for the uptake K_d values. Of the two types of K_d values, the desorption values are more important for risk or reactive transport modelling because they would constitute the rate limiting reaction in the subsurface environment, i.e., the desorption process is slower than the uptake process. Furthermore, it was shown that the type of iodine species added to the grout formulation impacted K_d. Iodine species ranked by their desorption K_d in grout prepared from Mix 1 are:



The ranking of desorption K_d for Mix 13 grout by iodine species was different:



It was also shown that grout formulation influenced iodine K_d values. Irrespective of which form of iodine was initially added to the grout mix, Mix 13.0 had greater desorption K_d values.

Table 19 compares the present values used in the SSW IDF data package with those values reported here. The ^{99}Tc K_d values measured here are about three to six times greater than those recommended for the oxidized conditions. The adsorption iodine K_d values measured in this study, Table 16, are approximately equivalent to those recommended for use under oxidizing conditions. However, the desorption K_d values are more appropriate for use in reactive transport modeling, and those values are generally appreciably greater than those recommended for either oxidizing or reducing conditions, Table 18. Furthermore, these data do not support the recommendation in Flach et al. (2016a) that there be different K_d values used for oxidizing and reducing conditions because the Mix 1 and Mix 13 K_d values did not significantly differ.

Table 19 Comparison of K_d values measured in this report vs. those recommended in the SSW IDF data package (Flach et al. 2016).

Radionuclide	Existing Recommendation K_d (mL/g) for Stage I/Stage II/Stage III (Flach et al., 2016b)		Measured K_d Value in this Report (mL/g)	Source of data from this Report
	Oxidized Conditions	Reducing Conditions		
Tc	0.8/0.8/0.8	1000/1000/1000	5.0 (a)	Figure 17
			2.8 (a)	Figure 18
I	4/8/2	n/a	3.0 (a)	Table 16, Mix 1, I^-
			3.1 (a)	Table 16, Mix 1, IO_3^-
			6.1 (d)	Table 18, Mix 1, I^-
			30.6 (d)	Table 18, Mix 1, IO_3^-
			32.3 (d)	Table 18 Mix 1, org-I
			2.3 (a)	Table 16 Mix 13, I^-
	n/a	0/2/0	2.8 (a)	Table 16 Mix 13, IO_3^-
			7.5 (d)	Table 18 Mix 13, I^-
			121.8 (d)	Table 18 Mix 13, IO_3^-
			42.1 (d)	Table 18 Mix 13, org-I

Note: (a) adsorption K_d , (d) desorption K_d

6.0 References

- Angus, M. J., and Glasser, F. P. (1985). The Chemical Environment in Cement Matrices. *Mat. Res. Soc. Symp. Proc.* **50**, 547-556.
- ASTM (C39/C39M – 15a). Standard Test Method for Compressive Strength of Cylindrical Concrete Specimens. West Conshohocken, PA.
- ASTM (C150-18). Standard Specification for Portland Cement. ASTM, West Conshohocken, PA
- ASTM (C490-11). Standard Practice for Use of Apparatus for the Determination of Length Change of Hardened Cement Paste, Mortar, and Concrete. West Conshohocken, PA.
- ASTM (C1733-10). Standard Test Method for Distribution Coefficients of Inorganic Species by the Batch Method. West Conshohocken, PA.
- ASTM (C 191-13). Standard Test Method for Time of Setting of Hydraulic Cement by Vicat Needle. West Conshohocken, PA.
- ASTM (C 232-04). "Standard Test Methods for Bleeding of Concrete." ASTM, West Conshohocken, Pennsylvania.
- ASTM (C 1679-09). Standard Practice for Measuring Hydration Kinetics of Hydraulic Cementitious Mixtures Using Isothermal Calorimetry. West Conshohocken, PA.
- ASTM (D 5084-10). Standard Test Methods for Measurement of Hydraulic Conductivity of Saturated Porous Materials Using a Flexible Wall Permeameter. West Conshohocken, PA.
- ASTM (D 6103 – 04). Standard Test Method for Flow Consistency of Controlled Low Strength Material (CLSM). West Conshohocken, PA.
- Baroghel-Bouny, V., Mainguy, M., Lassabatere, T., and Coussy, O. (1999). Characterization and identification of equilibrium and transfer moisture properties for ordinary and high-performance cementitious materials. *Cement and Concrete Research* **29**, 1225-1238.
- Brown, E. (2016). STATEMENT OF WORK Requisition #: 281842 Title: Solid Secondary Waste Form Development Rev. 1. Richland, WA.
- Brown, G. N., Peterson, R. A., and Russell, R. L. (2011). "Small-Column Cesium Ion Exchange Elution Testing of Spherical Resorcinol-Formaldehyde " Rep. No. PNNL 20603. Pacific Northwest National Laboratory, Oak Ridge, TN.
- Cantrell, K. J., Westsik, J. H., Serne, R. J., Um, W., and Cozzi, A. D. (2016). "Secondary Waste Cementitious Waste Form Data Package for the Integrated Disposal Facility Performance Assessment," Rep. No. RPT-SWCS-006, Rev. A. Pacific Northwest National Laboratory, Richland, WA.
- Cozzi, A. D., Daniel, W. E., Eibling, R. E., Hansen, E. K., Reigel, M. M., Swanberg, D. J., J. H. Westsik, J., Piepel, G. F., Lindberg, M. J., Heasler, P. G., Mercier, T. M., and Russell, R. L. (2013). "Supplemental Immobilization of Hanford Low-Activity Waste: Cast Stone Screening Tests," Rep. No. SRNL-STI-2013-00465. Savannah River National Laboratory, Aiken, SC.
- EPA (2009). "Technical Notes for EPA Method 901.1, Gamma Emitting Radionuclides in Drinking Water," Rep. No. EPA 901.1. U. S. EPA, Washington, DC.
- Flach, G. P., Kaplan, D. I., Nichols, R. L., Seitz, R. R., and Serne, R. J. (2016a). "Solid Secondary Waste Data Package Supporting Hanford Integrated Disposal Facility Performance Assessment " Rep. No. SRNL-STI-2016-00175. Savannah River National Laboratory, Aiken, SC.
- Flach, G. P., Kaplan, D. I., Nichols, R. L., Seitz, R. R., and Serne, R. J. (2016b). "Solid Secondary Waste Data Package Supporting the Hanford Integrated Disposal Facility Performance Assessment," Rep. No. SRNL-STI-2016-00175, Rev. 0. Savannah River National Laboratory, Aiken, SC.
- Freeman, E., Gao, Y.-M., Hurt, R., and Suuberg, E. (1997). Interactions of carbon-containing fly ash with commercial air-entraining admixtures for concrete. *Fuel* **76**, 761-765.
- Hartman, M. J., Morasch, L. F., and Webber, W. D. (2006). "Hanford Site groundwater monitoring for fiscal year 2005." Pacific Northwest National Laboratory (PNNL), Richland, WA (US).
- Hillel, D. (1971). "Soil and Water: Physical Principles and Processes," Academic Press, Inc., New York, NY.

- J.H. Westsik, J., GF Piepel, G. F., Lindberg, M. J., Heasler, P. G., Mercier, T. M., Russell, R. L., Cozzi, A. D., Daniel, W. E., Eibling, R. E., Hansen, E. K., Reigel, M. M., and Swanberg, D. j. (2013). "Supplemental Immobilization of Hanford Low-Activity Waste: Cast Stone Screening Tests," Rep. No. SRNL-STI-2013-00465. Savannah River National Laboratory, Aiken, SC.
- Kaplan, D. I. (2009). "Tc and Pu Distribution Coefficients, K_d Values, for the Saltstone Facility Performance Assessment," Rep. No. SRNL-TR-2009-00019. Washington Savannah River Company, Aiken, SC.
- Kaplan, D. I. (2016). "Geochemical Data Package for Performance Assessment Calculations Related to the Savannah River Site," Rep. No. SRNL-STI-2009-00473. Rev. 1. Savannah River National Laboratory, Aiken, South Carolina.
- Kaplan, D. I., Roberts, K., Coates, J., Siegfried, M., and Serkiz, S. (2008). "Saltstone and concrete interactions with radionuclides: Sorption (K_d), desorption, and reduction capacity measurements," Rep. No. SRNS-STI-2008-00045, Savannah River National Laboratory, Aiken, SC.
- Kay, R., Surman, J., and Shete, D. (2017). "DFLAW Solid Secondary Wastes - Phase 2 Review of UK ILW and LLW Immobilization," Rep. No. DBD/4909//PRJ/RP/004 Rev. C. DbD Limited, Cheshire, UK.
- Klemczak, B., and Batog, M. (2016). Heat of hydration of low-clinker cements. *Journal of Thermal Analysis and Calorimetry* **123**, 1351-1360.
- Kurdowski, W. (2014). "Cement and Concrete Chemistry," Springer, New York.
- Lafond, E., Cau Dit Coumes, C., Gauffinet, S., Chartier, D., Le Bescop, P., Stefan, L., and Nonat, A. (2015). Investigation of the swelling behavior of cationic exchange resins saturated with Na⁺ ions in a C3S paste. *Cement and Concrete Research* **69**, 61-71.
- Mualem, Y. (1976). A New Model for Predicting the Hydraulic Conductivity of Unsaturated Porous Media. *Water Resources Research* **12**, 513-522.
- Nichols, R. L., Seitz, R. R., and Dixon, K. L. (2017). "Solid Secondary Waste Testing for Maintenance of the Hanford Integrated Disposal Facility Performance Assessment - 2017," Rep. No. SRNL-STI-2017-00564. Savannah River National Laboratory, Aiken, SC.
- Nimmo, J. R., and Winfield, K. A., eds. (2002). "Water Retention and Storage: Miscellaneous Methods." Soil Science Society of America.
- NRC (1991). Waste Form Technical Position, Rev. 0. U. S. Nuclear Regulatory Position.
- Ochs, M., Mallants, D., and Wang, L. (2016). "Radionuclide and Metal Sorption on Cement and Concrete," Springer, Heidelberg.
- Olliver, J. P., Maso, J. C., and Bourdette, B. (1995). Interfacial Transition Zone in Concrete. *Advanced Cement Based Materials* **2**, 30-38.
- Payá, J., Monzó, J., Borrachero, M. V., Perris, E., and Amahjour, F. (1998). Thermogravimetric Methods for Determining Carbon Content in Fly Ashes. *Cement and Concrete Research* **28**, 675-686.
- R Development Core Team (2017). R: A language and environment for statistical computing. R Foundation for Statistical Computing, Vienna, Austria.
- Scrivener, K. L., and Nemati, K. M. (1995). The Percolation of Pore Space in the Cement Paste/Aggregate Interfacial Zone of Concrete. *Cement & Concrete Research* **26**, 35-40.
- Serne, R. J., Westsik, J. H., Williams, B. D., Jung, H., and Wang, G. (2015). "Extended Leach Testing of Simulated LAW Cast Stone Monoliths." Pacific Northwest National Lab.(PNNL), Richland, WA (United States).
- Stumm, W., and Sulzberger, B. (1992). The cycling of iron in natural environments: considerations based on laboratory studies of heterogeneous redox processes. *Geochimica et Cosmochimica Acta* **56**, 3233-3257.
- Snyder, K. A., Winslow, D. N., Bentz, D. P., and Garboczi, E. J. (1992). Effects of interfacial zone precolation on cement based composite transport properties. *Materials Research Society Symposium Proceedings* **245**, 265-270.
- Tomlinson, M. (2016). American Rock Products 4257020-Perma Fix Grout 2500 PSI[0]. (R. L. Nichols, ed.), Richland, WA.

- Um, W., Jung, H. B., Wang, G., Westsik, J. H., and Peterson, R. A. (2013). "Characterization of Technetium Speciation in Cast Stone," Rep. No. PNNL-22977. Pacific Northwest National Laboratory.
- Um, W., and Serne, R. J. (2005). Sorption and transport behavior of radionuclides in the proposed low-level radioactive waste disposal facility at the Hanford site, Washington. *Radiochimica Acta* **93**, 57-63.
- Um, W., Valenta, M. M., Chung, C.-W., Yang, J., Engelhard, M. H., Serne, R. J., Parker, K. E., Wang, G., Cantrell, K. J., and Westsik Jr, J. (2011). "Radionuclide Retention Mechanisms in Secondary Waste-form Testing: Phase II," Rep. No. PNNL-20753. Pacific Northwest National Laboratory, Richland, WA.
- Um, W., Yang, J.-S., Serne, R. J., and Westsik, J. H. (2015). Reductive Capacity Measurement of Waste Forms for Secondary Radioactive Wastes. *Journal of Nuclear Materials* **467**, 251-259.
- van Genuchten, M. T. (1980). A Closed-form Equation for Predicting the Hydraulic Conductivity of Unsaturated Soils. *Soil Science Society of America Journal* **44**, 892-898.
- Williams, C. D., and Carbone, P. (2015). A classical force field for tetrahedral oxyanions developed using hydration properties: The examples of pertechnetate (TcO_4^-) and sulfate (SO_4^{2-}). *The Journal of Chemical Physics* **143**, 174502.
- Winslow, D. N., and Liu, D. (1990). The pore structure of cement paste in concrete. *Cement and Concrete Research* **20**, 227-235.
- WRPS (2016). "Test Specification for the Low-Activity Waste Pretreatment System Full-Scale Ion Exchange Column Test and Engineering-Scale Integrated Test (Project T5L01)," Rep. No. RPP-RPT-58683, Rev. 2, Richland, WA.
- Zhang, S., Schwehr, K. A., Ho, Y. F., Xu, C., Roberts, K. A., Kaplan, D. I., Brinkmeyer, R., Yeager, C. M., and Santschi, P. H. (2010a). A Novel Approach for the Simultaneous Determination of Iodide, Iodate and Organo-Iodide for I-127 and I-129 in Environmental Samples Using Gas Chromatography-Mass Spectrometry. *Environmental Science & Technology* **44**, 9042-9048.
- Zhang, S., Schwehr, K. A., Ho, Y. F., Xu, C., Roberts, K. A., Kaplan, D. I., Brinkmeyer, R., Yeager, C. M., and Santschi, P. H. (2010b). A Novel Approach for the Simultaneous Determination of Iodide, Iodate and Organo-Iodide for I-127 and I-129 in Environmental Samples Using Gas Chromatography-Mass Spectrometry. *Environmental Science & Technology* **44**, 9042-9048.

Distribution:

T. B. Brown, 773-A
M. E. Cercy, 773-42A
D. A. Crowley, 773-43A
D. E. Dooley, 773-A
A. P. Fellingner, 773-42A
S. D. Fink, 773-A
C. C. Herman, 773-A
K. L. Dixon, 773-42A
D. I. Kaplan, 773-42A
K. A. Hill, 999-W
C. E. Burckhalter, 999-W
C. A. Langton, 773-42A
J. E. Hyatt, 773-A
L.T. Reid, 773-42A
B. B. Looney, 773-42A
D. A. McGuire, 773-42A
N. V. Halverson 773-42A
F. M. Pennebaker, 773-42A
G. N. Smoland, 773-42A
A. L. Washington, 773-42A
W. R. Wilmarth, 773-A
Records Administration (EDWS)